

Re-evaluation of characters in Apolemiidae (Siphonophora), with description of two new species from Monterey Bay, California

STEFAN SIEBERT¹, PHIL R. PUGH², STEVEN H. D. HADDOCK³ & CASEY W. DUNN¹

¹*Department of Ecology and Evolutionary Biology, Brown University, Providence, Rhode Island, 02912, United States of America*

²*National Oceanography Centre, Southampton, SO14 3ZH, UK*

³*Monterey Bay Aquarium Research Institute, Moss Landing, California, 95039, United States of America*

Abstract

Siphonophores are polymorphic planktonic marine Cnidarians. The family Apolemiidae is sister to all other species of physonect and calycothorac siphonophores. Although this enigmatic group arguably includes the longest animal species on the planet, their colony-level organization and growth patterns are not well understood. Here we describe two new apolemiid species: *Apolemia lanosa* sp. nov. and *A. rubriversa* sp. nov. We provide detailed descriptions of zooid budding and the organization of mature zooids within the siphosome. Our findings reveal that at least two distinct general patterns of siphosomal organization are found in different *Apolemia* species. In the first pattern, dispersed organization, zooids independently attach directly to the siphosomal stem. In the second pattern, pedunculate organization, only the gastrozooid is attached directly to the stem, and the other zooids of the cormidium branch from its peduncle. This diversity within *Apolemia* indicates that fundamental aspects of zooid budding and organization are homoplastic within Siphonophora, as both patterns are also found in other siphonophores. The observations presented here greatly clarify the interpretation of diagnostic characters within Apolemiidae, bear on the status of the three previously described species, provide critical detail for understanding the diversity of colony-level organization in siphonophores, and establish a foundation for the description of additional apolemiid species.

Key words: Cnidaria, Hydrozoa, Siphonophora, Apolemiidae, Apolemia, Cormidial organization, Colony formation

Introduction

Siphonophores are free-swimming colonial animals that belong to Hydrozoa (Cnidaria). Most siphonophores are entirely pelagic, and they are abundant in the midwater of all oceans (Mackie *et al.* 1987). Each siphonophore colony consists of multiple physiologically integrated bodies, or zooids, each of which is homologous to a solitary free-living animal. Each zooid is specialized to perform a particular function, such as locomotion, feeding, protection, or reproduction. Siphonophores are often very fragile, and the study of their systematics has been largely based on a small number of characters that can be described from dissociated specimens (Totton 1965). These commonly described features include the morphology of the nectophores (swimming zooids), bracts (protective zooids), and the tentacles of gastrozooids (feeding zooids). New technologies including remotely operated underwater vehicles, blue-water SCUBA diving and submersibles have made it possible to collect many siphonophore species intact for the first time (Haddock 2004). This allows for the description of a much broader set of characters than was previously possible, including the organization of zooids within the colonies (Dunn & Wagner 2006).

The zooids of most siphonophores are organized along an elongate linear stem. The stem can have one or two main budding zones, which are the sites of both stem elongation and the addition of new zooids throughout the life of the colony (Carré & Carré 1995). All siphonophores have a siphosome, a region of the colony that bears gastrozooids, bracts, and sexual zooids, among others, and that is produced by the siphosomal growth zone. The zooids of the siphosome are organized in repeating patterns, each iteration of which is called a cormidium. Siphonophores have been traditionally divided into three major groups: Cystonectae, Physonectae and

Calycophorae (Fig. 1A, Totton 1965). These groups differ in the presence of two conspicuous characters. The first is the pneumatophore, a gas filled float found only in Cystonectae and Physonectae. The second is the nectosome, a region of the colony specialized for locomotion, which is found only in species of Physonectae and Calycophorae. Like the siphosome, the nectosome has its own growth zone. Molecular data indicate that Cystonectae are monophyletic, but based on 18S rRNA Physonectae is paraphyletic and gave rise to Calycophorae (Collins 2002; Dunn *et al.* 2005). The clade comprising “Physonectae” and Calycophorae is named Codonophora (Dunn *et al.* 2005).

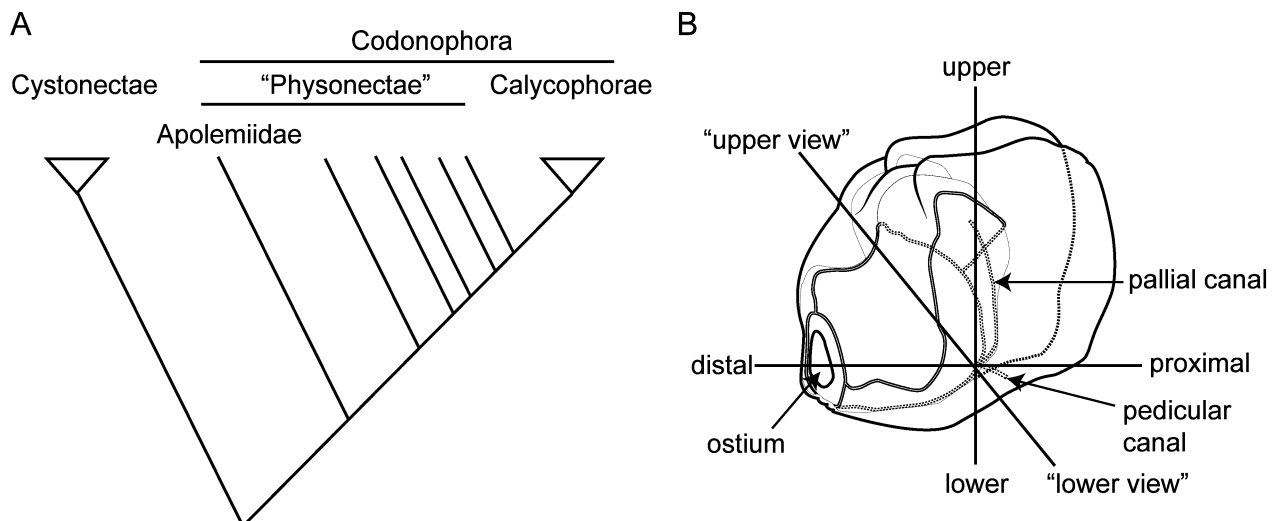


FIGURE 1. (A) Phylogenetic position of Apolemiidae within Siphonophora (after Dunn *et al.* 2005). (B) Schematic lateral view of an apolemiid nectophore, showing the major axes and the directions of the “upper” and “lower” views used in graphic presentations in this study.

Apolemiidae is sister to all other species of Codonophora (Fig. 1A; Dunn *et al.* 2005). This phylogenetic position makes the study of Apolemiidae critical to understanding the evolution of many features of siphonophore structure and development. In addition, apolemiids have many unique attributes that make them of particular interest, including the ability to grow to lengths in excess of 30 meters (Mackie *et al.* 1987) and a complex nectosome. Even so, they have remained among the most poorly known groups of siphonophores. To date three apolemiid species have been described, *Apolemia uvaria* Lesueur, 1815, *Ramosia vitiazii* Stepanjants, 1967 and *Tottonia contorta* Margulies, 1976. In this study we describe two new apolemiid species, re-evaluate diagnostic characters for the group, and discuss the state of the genus *Apolemia*. For reasons discussed below, we ascribe both new species to the genus *Apolemia*. In addition, for the first time in Apolemiidae, we describe the structure of the growth zones and details of the colony-level organization of the zooids. The insights provided here build a foundation for future systematic studies of Apolemiidae (which is thought to include at least 15 further undescribed species), and provide insight into the development and evolution of Siphonophora.

Material and methods

Specimens were collected in the vicinity of Monterey Bay, California, and adjacent waters by the ROVs *Doc Ricketts* (D), *Tiburon* (T) (both deployed from the R/V *Western Flyer*) or ROV *Ventana* (V) (deployed from the R/V *Point Lobos*). The four specimens (from dives D327, D329, D331, D423) described in detail here were relaxed in MgCl₂, partially dissected, and pinned out in a Petri dish coated with Sylgard 184 (Dow Corning Corporation). A thin layer of Sylgard allows for the use of insect pins (Austerlitz Insect Pins, 0.2mm, Fine Science Tools) to fixate tissue in the dish. Extensive observations, including photo-documentation, were made on living specimens and later on fixed material. Specimens were preserved in 5% buffered formalin. Specimens D195 and V908 were fixed directly in 5% buffered formalin without prior relaxation. Samples from the siphosomal stem were snap frozen for DNA extraction prior to fixation in all cases except for specimen V908. The nematocyst complement was documented after mounting fixed tissue samples in 80% glycerol. Minimum, maximum and mean measurements

are provided as well as the number of measurements taken (Table 4). The orientation of the nematocysts in the tissue sample did not allow for length measurements in all cases.

To make scanning electron microscope (SEM) images of the siphosomal organization of specimen D331, tissue preserved in 5% buffered formalin was fixed with 3.5% glutaraldehyde in 0.05 M sodium cacodylate buffer, pH 7.4, for 18h at 4°C. After washing with 0.075 M sodium cacodylate buffer for 30 min, the specimen was postfixed with 1% OsO₄ in 0.075 M sodium cacodylate buffer for 2 h at room temperature. After additional washing with 0.075 M sodium cacodylate buffer for 30 min, the tissue was dehydrated in an EtOH series. Samples were critical point dried, sputtered with gold and examined with a Hitachi 2700 SEM.

Several gene regions were sequenced to aid in identification and to facilitate future phylogenetic analyses of *Apolemia* when more species are described. Total DNA was extracted from four specimens (D195, D327, D329 and D331) with Trizol (Life Technologies). The following partial gene sequences were amplified: 16S (primer from Cunningham & Buss 1993), 18S (primer from Medlin *et al.* 1988), 28S (primer F63sq from Medina *et al.* 2001 and primer LSU D1,D2 rev1 from Sonnenberg *et al.* 2007), COI (primer LCO1490 from Folmer *et al.* 1994 and HCO-Med-2414 from Bucklin *et al.* 2010) and Histone 3 (primer H3-F and H3-R from Colgan *et al.* 2000). Sequences were submitted to GenBank (Accession Nos. KF214712-KF214721). Sequence differences between the two species were 0.4% (SSU), 1.0% (28S), 2.2% (16S), 4.6% (H3) and 5.2% in case of COI.

An *Apolemia uvaria* specimen was borrowed from the Natural History Museum, London (BMNH 1952-9-23-96). This specimen was collected by A. K. Totton in Villefranche-sur-Mer, France, on April 23rd in 1949. A nectophore of the type specimen of *Tottonia contorta* taken by Petr Lebedev from 660-583-0m at Station 11 (07°39'N 87°54'E); most of the *Tottonia* paratype specimen (collected in the equatorial region of the Pacific Ocean (01°30.5'-01°01.4'S, 97°00'-97°02.7'W) by the RV *Akademik Kurchatov* on 14 Jan 14th 1974 using a plankton net at St. 1454, fishing depth 180 m (series no. 50, 2055 hrs)); and the paratype specimen of *Ramosia vitiazii* (collected from 1765 m at 53°04'N 146°10.5'E by the *Vitiaz* on 21st September 1951) were made available through the kindness of Sofia Stepanjants. These specimens are held at the Zoological Academy of Sciences, St Petersburg with registration Nos. 9228, 2/9228 and 319902, respectively.

Terminology. We describe orientation, views, and axes following the terminology of Haddock *et al.* (2005). Due to their shape, apolemiid nectophores naturally sit in the dish at an angle such that the upper and lower surfaces do not face directly up or down, but instead are inclined at an angle of approximately 45° (Fig. 1B). Nonetheless, we will still refer to these views as “upper” and “lower”.

Nectosomal zooids in between nectophores had originally been called palpons (“Fühler” [feeler], “Taster”) (Kölliker 1853; Leuckart 1854). More recently, (Totton 1965) referred to them as tentacles, and they were interpreted as being homologous to the aboral tentacles of other hydrozoans (Leloup 1954). However, we find that these structures have well-defined gastric cavities and their nematocyst complements, as presented in this study, show similarities to the ones of gastrozooids and siphosomal palpons and major differences to those of the tentacles and palpacles. Furthermore *in vivo* behavior shows feeling/sensing activity in a very similar way comparable to that observable for siphosomal palpons. As feeding function has not been reported for these accessory zooids, we here choose to call them nectosomal palpons. Small buds that may correspond to vestigial nectosomal palpons have also been found in *Bargmannia elongata* Totton by Dunn (2005). This suggests that nectosomal palpons may be a synapomorphy of Codonophora that has been greatly reduced or entirely lost in representatives other than the apolemiids.

According to Totton (1965, p. 35), peduncle and pedicel are interchangeable terms used for the foot-stalk of attachment of gastrozooids, palpons, nectophores and gonophores. Mapstone (2009), however, defined pedicel as “stalk of a zooid” and made no use of the term peduncle. In this study we consistently use the term peduncle. In the case of a gonodendron, which is not an independent zooid, we use the term stalk to describe the structure to which the gonophores are attached via individual peduncles.

Abbreviations used in figures

aw: axial wings

b: bract

bas: basigaster

bl: bracteal lamella

dgb: developing gastrozooidal bract
div: diverticulum
dlc: distal loop lateral canal
dpb: developing palpon bract
dpc: developing palpon cluster
g: gastrozooid
go: gonozooid
h: siphosomal horn
lc: lateral canal
lf: lateral furrow
loc: lower canal
m: mastigophore
ma: macroisorhizas
mi: microisorhizas
n: nectophore
nc: nucleus
nml: nectophoral muscular lamella
np: nectosomal palpon
nps: nectophoral palpon scar
ns: nectosac
nst: nectosomal stem
orc: ostial ring canal
os: ostium
p: palpon
pa: palpacle
pac: pallial canal
pc: palpon cluster
pd: peduncle
ped: pedicular canal
plc: proximal loop lateral canal
pn: pneumatophore
rc: refractile cell
sbz: siphosomal budding zone
sg: secondary gastrozooid
sp: stem sphincter
sst: siphosomal stem
st: stenoteles
tb: thrust block
uc: upper canal
ui: unidentified capsule

Results

Systematics

Family Apolemiidae Huxley, 1859

Diagnosis. Colony linear and having ventral nectosome with many similar nectophores and one to several nectosomal palpons associated with each nectophore; nectophores ridgeless; dioecious; gastrozooid tentacles simple and without tentilla.

Genus *Apolemia* Eschscholtz, 1829

Apolemia lanosa sp. nov.

Material examined: Doc Ricketts Dive D327-D4, 4 Dec 2011, 35°56'N, 122°55'W, depth 636 m.

Doc Ricketts Dive D329-SS6, 6 Dec 2011, 36°6.99'N, 122°54.01'W, depth 1030 m.

Doc Ricketts Dive D423-D12, 1 Oct 2012, 36°15.02'N, 123°9.98'W, depth 1325 m.

Due to their lengths, only the anterior parts of the specimens D327-D4 and D329-SS6, including the pneumatophore, nectosome, and anterior siphosome, could be collected. A posterior part of the siphosomal stem bearing gonophores was collected for D423-D12. *In situ* high definition (HD) videos were recorded for specimen D327-D4 and D329-SS6, and are provided as supplementary video (Supplementary video).

Holotype: The specimen D327-D4 has been designated as the holotype and specimens D329-SS6 and D423-D12 as paratypes. All three specimens have been deposited at the National Museum of Natural History, Smithsonian Institution, Washington DC (USNM 1207944, USNM 1207945, and USNM 1207946, respectively). All of the following observations were made on the holotype and on living tissue, unless explicitly stated otherwise.

Diagnosis. Large nectophores with patches of nematocysts covering their upper and upper-lateral sides. Refractile cells scattered in and around these patches. No distinct diverticula on lateral radial canals. Number of nectosomal palpons per nectophore increasing in posterior direction, with an observed maximum of four. Bracts with similar patches and refractile cells on distal two-thirds of upper surface. Siphosomal growth zone with inconspicuous horn. Cormidia dispersed, each with one type of palpon. Cormidia with one primary gastrozooid and an increasing number of secondary gastrozooids in more posterior parts of the colony.

General appearance: The orange-white tinge of the siphosome, with deep red gastrozooids, contrasted with the complete lack of color in the nectosome (Fig. 2A,C). The zooids of the siphosome were densely packed, without any obvious bare stem between them. The bracts were conspicuous. Bracts, gastrozooids and numerous palpons gave the siphosome a relatively thick and well-defined fleece-like outline (Supplementary Video).

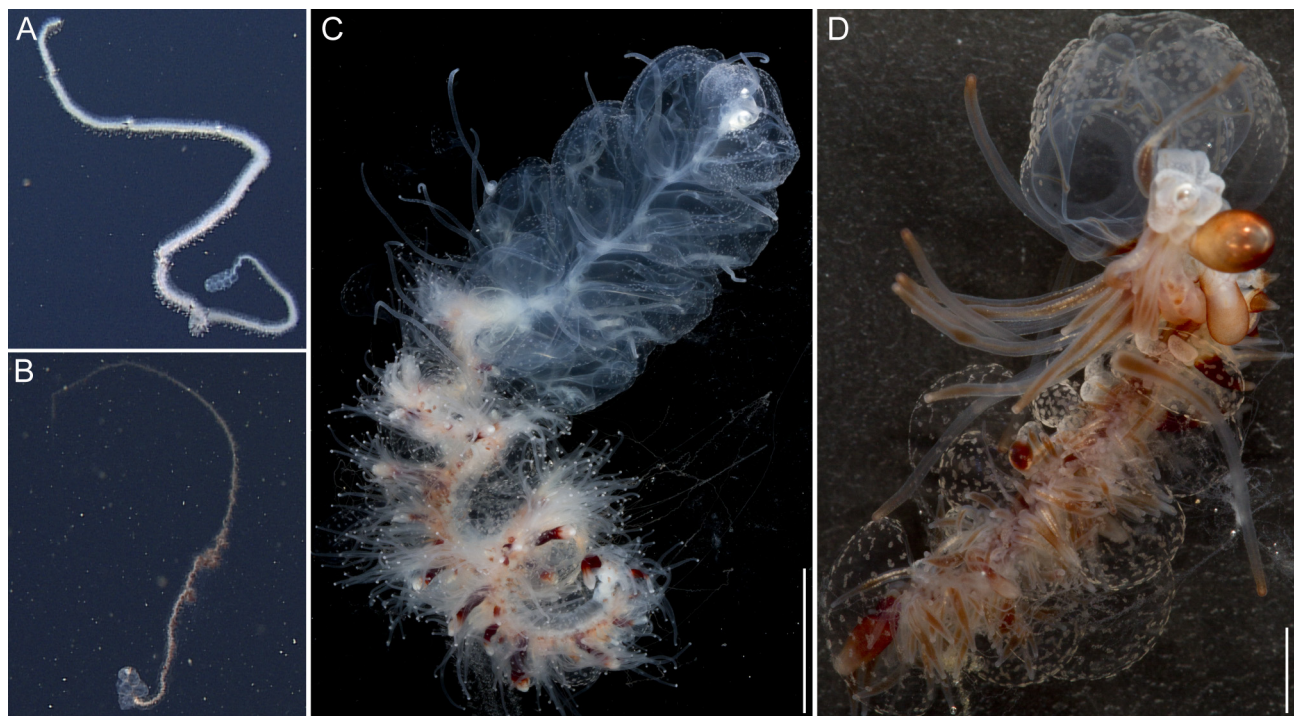


FIGURE 2. (A–B) *In situ* photographs of holotype specimens. (A) *Apolemia lanosa* sp. nov., approximate length 2 m. (B) *Apolemia rubriversa* sp. nov., approximately 1.2 m in length. (C–D) Anterior regions of the collected, unfixed specimens of (C) *A. lanosa*, which had already lost most of its bracts (Scale bar 2 cm); and (D) *A. rubriversa*, which most of its mature nectophores detached (Scale bar 2.5 mm).

Pneumatophore: The pneumatophore of the holotype specimen was ovoid, 2.2 mm in height and 1.4 mm in maximum diameter, with a silvery appearance and no obvious pigmentation (Fig. 3A).

Nectosome: The colorless nectosome of the holotype measured 6 cm in length after relaxation (Figs. 2C, 3). The nectophores were attached, in a single line, on the ventral side of the stem. *In vivo* the nectosomal stem was twisted. A 180° turn of the stem between two adjacent nectophores resulted in a biserial arrangement of nectophores (Fig. 3D). Fourteen attachment lamellae were found on the nectosome of the holotype, including the ones with nectophores still attached. The youngest nectophores, toward the anterior end of the nectosome, were each accompanied by a single nectosomal palpon (Fig. 3B). Further to the posterior, with the increasing age of the nectophores, the number of palpons per nectophore increased, such that there were four associated with the oldest nectophore of the holotype (Fig. 3C). The nectosomal palpons lacked a palpacle and were attached directly to the stem to the posterior end and, in ventral view, left of the nectophore lamella. In a relaxed state these palpons were about three times as long as the associated nectophore. Nematocysts, occurring as small opaque spots, were scattered over the surface of the palpon, but were mainly concentrated in its distal region.

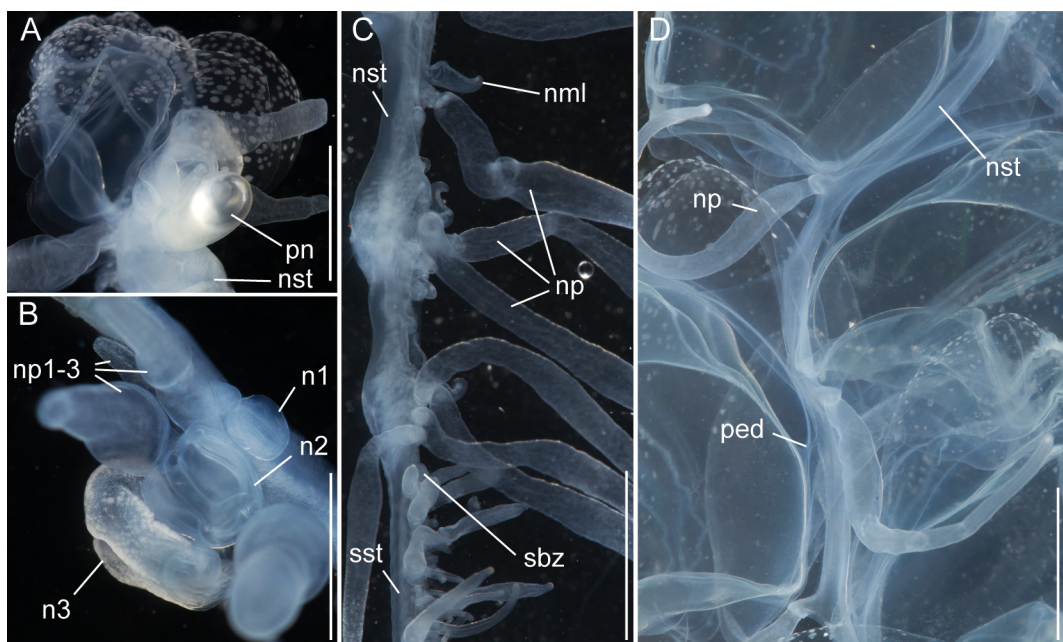


FIGURE 3. *Apolemia lanosa* sp. nov. Nectosome of the holotype specimen (live, A–C) and specimen from Doc Ricketts dive D329 (live, D). (A) Nectosomal growth zone with young nectophores still attached. The pneumatophore is at center and posterior at the bottom. (B) Close-up of the nectosomal growth zone. The pneumatophore is just out of frame to the upper left. (C) Posterior part of nectosome and anterior part of siphosome after removal of nectophores, with nectosomal palpons still attached to the ventral side of the stem. Anterior is up. (D) Close-up of twisted nectosomal organization with nectophores still attached. Anterior is up. Scale bars in A–D 5 mm.

Nectophores: No sign of any pigmentation was seen on the nectophores (Figs. 2C, 3A, 4A–C, 4G–U). The largest nectophore of the holotype specimen had a length of 21.4 mm and a width of 17.6 mm (Fig. 4P). Living and fixed nectophores differed in appearance. In general, furrows tended to be more pronounced in fixed tissue. The appearance of a fixed nectophore varied with the presentation in the dish (compare Figs. 4R, 4S). *In vivo*, the state of contraction influenced nectophore appearance, which in consequence might influence the resulting nectophore morphology at the time point of fixation (compare Figs. 4T, 4U). The youngest nectophores (n1–2, Fig. 3B) within the growth zone had very prominent canals and a translucent epidermis, while older ones (n3) were slightly opaque. The upper and upper lateral surfaces of the latter were densely covered with nematocysts, which were organized into defined patches in older nectophores (Figs. 3A, 4A–C, 4G–U). The distance between these patches was correlated with the size of the nectophore (Figs. 4 G–P). This suggests that the patches have a similar total area through the course of maturation, and that the patches become further separated as the nectophore grows. On the axial wings of more mature nectophores these patches tended to be more rounded, while those on the main body of the nectophore were more elongate (Figs. 4A–C). In addition, refractile cells were sparsely scattered between and within these patches of nematocysts.

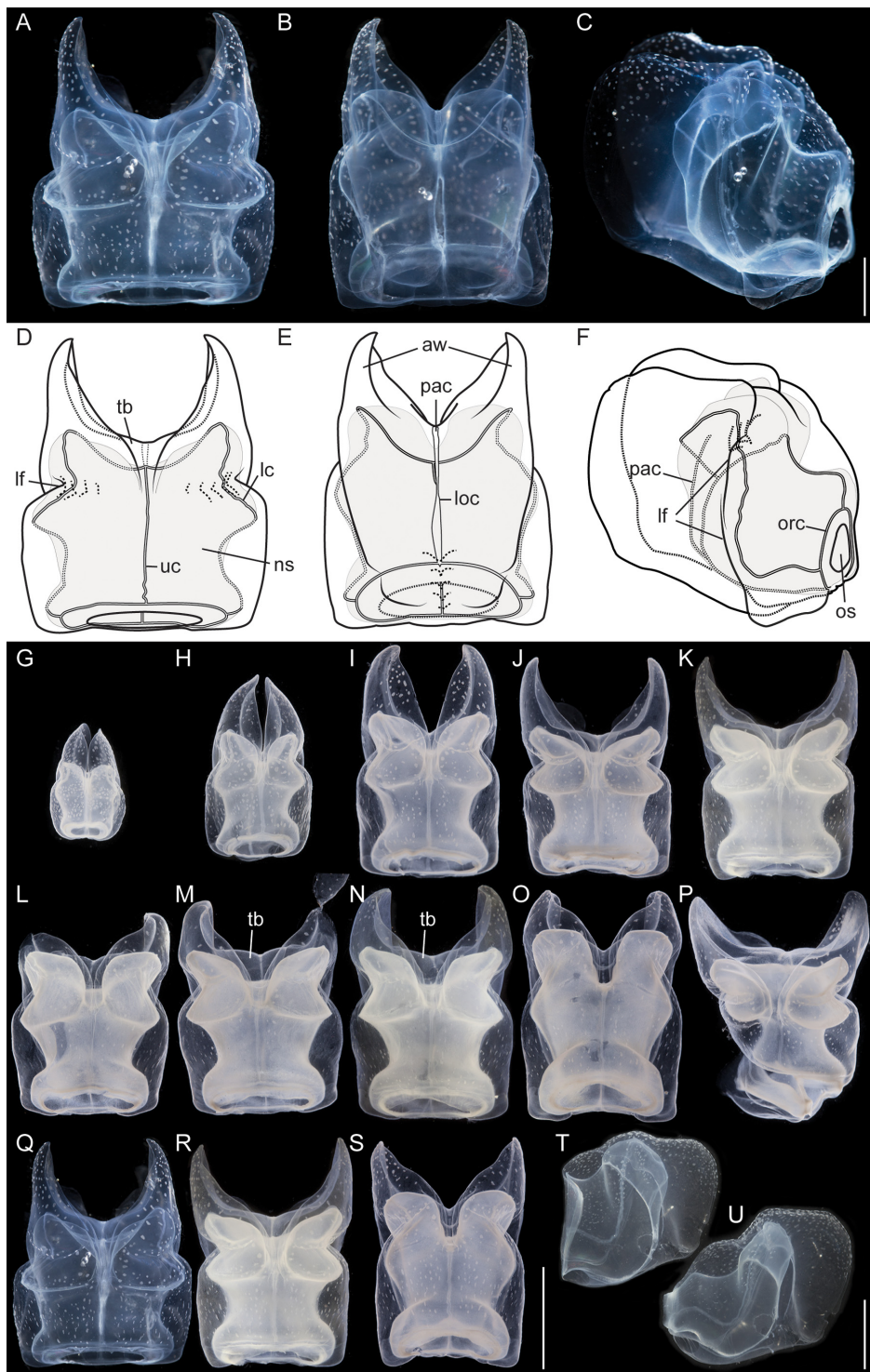


FIGURE 4. *Apolemia lanosa* sp. nov. Medium sized nectophore from the holotype specimen (living, A–C). Photographs and drawings of upper (A, D), lower (B, E), and lateral (C, F) views. Scale bar (5 mm) in C applies to figures. (G–S) Photographs of “upper” view of nectophores from the holotype and lateral view of the paratype specimen (T–U). All the nectophores had been fixed apart from those shown in Q, T and U. (G–P) Photographs showing change in nectophore morphology and proportions during growth. Axial wings were close to each other in young nectophores and widely apart in mature ones. The thrust block was well developed and the axial wings were proportionally shorter in older nectophores. (Q–S) Photographs of the same nectophore after relaxation while living (Q), and after fixation (R–S). Appearance of nectophore morphology in fixed state varied significantly with viewing angle and how the nectophore was presented in the dish. In S the nectophore was gently stretched in the longitudinal direction. T–U show the same nectophore, while living, of specimen D329-SS6 freshly detached from the stem in an uncontracted (T) and fully contracted (U) state. Scale bar (1 cm) in (S) applies to nectophores in G–S. Scale bar (1cm) in (U) applies to T–U.

The large, flared axial wings occupied about one third the total length of the younger nectophores and about one fourth of the mature ones (Figs. 4G–P). The central thrust block was very narrow in early nectophore development and well developed in mature nectophores (Fig. 4G–P). A broad, relatively shallow lateral furrow extended almost vertically up each side of the nectophore, from the lateral margins of the lower surface to the upper surface. In most of the nectophores it reached the inner, upper margins of the axial wings (Figs. 4A,D, 4G–P). On the lower surface of the nectophore, i.e. that which is closest to the stem, the lower margins of the axial wings began to approach each other from above the level of the proximal side of the nectosac, but each petered out well short of the mid-line (Fig. 4B,E). There was a pair of small, slightly thickened cushions of mesoglea on the lower surface of the nectophore that delineated a shallow lower furrow, overlying the lower radial canal. The nectosac mostly filled the main body of the nectophore (Fig. 4). It was broadest just above the ostium and at about half of its length.

No descending pallial canal was present. From its origin from the pedicular canal, the ascending pallial canal ascended towards the top of the thrust block and ended at about two thirds of the total height of the nectosac (Fig. 4C,F). The lower radial canal was frequently torn in the region where it ran in close contact with the lower part of the muscular attachment lamella, after which it passed along the base of the lower groove to reach the ostial ring canal (Fig. 4B,E).

The upper radial canal gave rise symmetrically to the lateral radial canals close to the mid-height of the proximal side of the nectosac (Fig. 4 E,F). It then continued over onto the upper side of the nectosac and to the ostial ring canal. Although straight for the most part, just above the ostium it had a series of small bends (Fig. 4D). The lateral radial canals, from their point of origin, curved away from the midline and upwards to the apico-lateral margins of the nectosac and passed, slightly undulating, over onto the upper surface before curving outwards to run obliquely downwards toward the lower surface of the nectosac, but curving upwards again before reaching that surface and then bending to run directly to the ostium, reaching it at about half its height (Fig. 4D, F). No distinct diverticula could be observed on the lateral canals but occasionally small protrusions were observed.

Siphosome: The full length of the siphosome prior to collection was about 2m in the state of relaxation as pictured in Fig. 2A. After relaxation, the siphosome of the partial holotype fragment that was collected measured 12 cm in length (Fig. 2C). The stem and the attached palpons were milky-white, while the basal region of the palpacles had a faint red tinge. The body columns of the gastrozooids were of deep red color.

Siphosomal growth zone and early zooid development: The siphosomal growth zone had an inconspicuous horn that pointed in the anterior direction (Figs. 5, 6A). Gastrozooid buds originated on the horn. Gastrozooid morphology, with a peduncle, ring-like basigaster, and proboscis was apparent at very early stages (Fig. 5B). These primary gastrozooids were alternately displaced to the left and right slightly off the ventral midline resulting in a biserial organization that was most conspicuous in the youngest cormidia (Fig. 5B). To the anterior of the gastrozooid peduncle, attached directly to the siphosomal stem, was a compound palpon bud. Each compound palpon bud gave rise to a palpon cluster. Key aspects of palpon morphology were in place by cormidium eight (Fig. 5B). Developing palpacles had an opaque appearance (Fig. 6B), first of a yellowish coloration, while older palpacles showed an intense orange at their proximal ends (Fig. 6C, Fig. 8A,E). In the case of the gastrozooids, no tentacle formation could be observed during early zooid development. Palpacle formation, therefore, preceded gastrozooidal tentacle formation. Bract formation was first observed in association with gastrozooids (Fig. 6B). Each gastrozooid was accompanied by a single bract attached to the ventral midline just to the posterior of the gastrozooid (Fig. 6B). This gastrozooidal bract marked the posterior end of each cormidium. A stem sphincter is located just posterior to the gastrozooidal bracts (Fig. 6C). Removal of the gastrozooidal bract left a curled attachment lamella (Fig. 6D,E). A second type of bract was associated with the palpons. These were located laterally. The first of these lateral bracts to form arose toward the posterior end of each palpon clusters. As the palpon clusters grew, more bracts were added in the anterior direction. In older parts of the colony new secondary gastrozooids formed in between primary gastrozooids (Fig. 6F) indicating that the distance between the latter increased with the age of the cormidium. The addition of new zooids, therefore, occurred along the siphosomal stem and was not restricted to the siphosomal growth zone.

Bracts: As the ROV approached, the colony rapidly began to autotomize its mature bracts, and so it was difficult to document their *in vivo* arrangement. In addition, a large fraction of the bracts were lost during the sampling procedure. Thus, by the time the colony was examined, few mature bracts remained attached directly to the siphosomal stem. Developing gastrozooid and palpon lateral bracts were very similar, though they became more

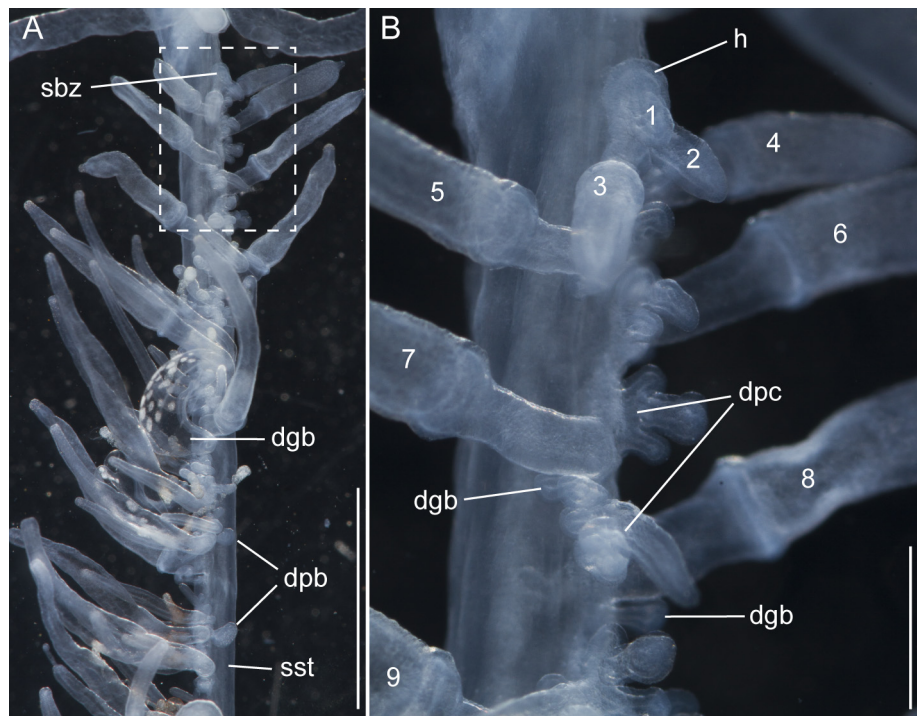


FIGURE 5. Anterior portion of *Apolemia lanosa* sp. nov. siphosome, including the siphosomal growth zone, photographed while living. Ventral view, anterior is up. (A) Scale bar 5 mm. (B) Close-up of the first eight cormidia from the region framed by the dashed box in (A). Scale bar 1 mm. Numbers indicate primary gastrozooids starting with the youngest.

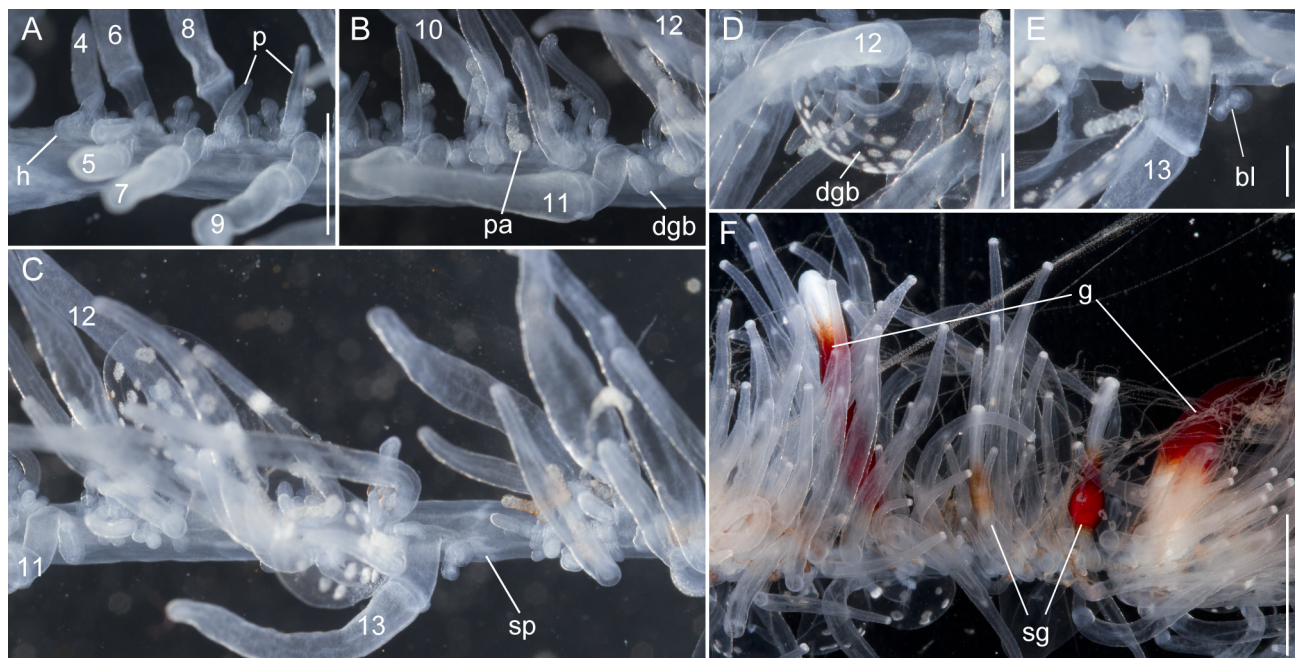


FIGURE 6. *Apolemia lanosa* sp. nov. Cormidial organization of the holotype specimen (live). Anterior is to the left, ventral is up. (A–C) Sequential photographs of the anterior part of siphosome. Scale bar in (A) 2 mm applies to (A–C). (B) Early palpacles and a young bract associated with a primary gastrozooid. (C) Sphincter region posterior to a primary gastrozooid. (D) Developing gastrozooidal bract associated with primary gastrozooid 10. Scale bar 1 mm. (E) Curled bracteal canal and attachment lamella that remained after detachment of the gastrozooidal bract. Scale bar 1 mm. (F) Secondary gastrozooids intercalated between primary gastrozooids in older cormidia. Scale bar 5 mm.

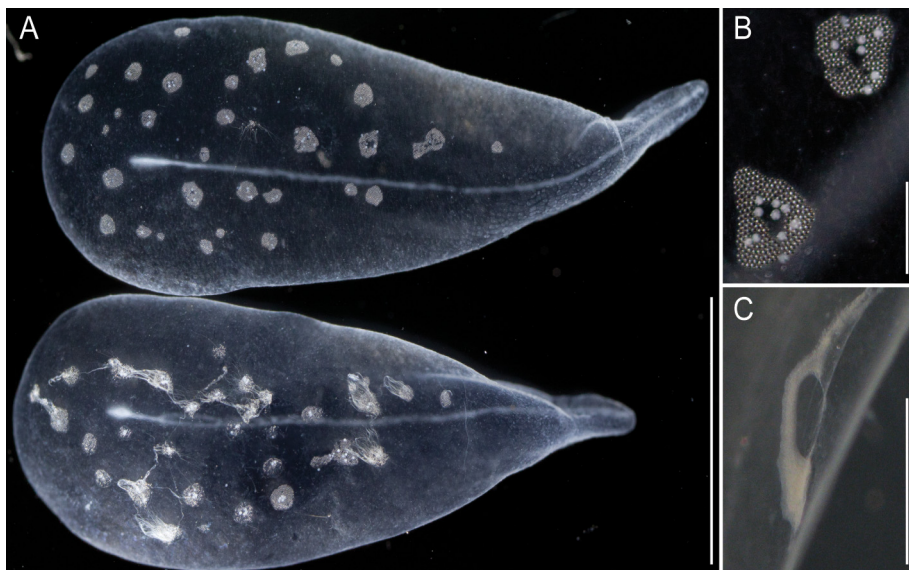


FIGURE 7. *Apolemia lanosa* sp. nov. Gastrozooid bracts of the holotype specimen (fixed). (A) Upper view of bracts. Bract at bottom with discharged nematocyst tubules visible. Scale bar 5 mm. (B) Close-up of nematocyst patches. Refractile cells appear as larger white specks within nematocyst patches. Scale bar 400 µm. (C) Distal end of bracteal canal bends into the mesoglea and back towards the lower bract surface (end of canal at bottom). Scale bar 1 mm.

distinct as they matured. Mature gastrozooid bracts were very elongate and straight without an obvious keel (Fig. 7A). Mature palpon bracts tended to be more ovoid in shape and more curved, and they tapered to form a more rounded proximal end on the upper surface. In this case the mesoglea was generally thicker and, on the lower surface, it bulged out slightly to form a small, but distinct, keel. The bracteal canal arose from the proximal end of the bract. Nematocyst patches were scattered over the distal two-thirds of the upper side of the bracts (Fig. 7A). As observed in the case of nectophores individual large refractile cells could be found scattered between and within these nematocyst patches (Fig. 7B). In all bracts the bracteal canals extended distally along the lower surface in the mid-line. At their distal ends they bent into the mesoglea and then back towards the lower surface (Fig. 7A,C). However, the distinctiveness of this arch varied considerably, and it was in many cases difficult to detect.

Palpons: Only a single type of siphosomal palpon was observed. The maximum length of the palpon was 22 mm when fixed. *In vivo*, however, palpons could reach twice the length of gastrozooids (Fig. 2C). Palpons were slightly opaque and of a milky-white color, with a more opaque, white region at their distal ends (Figs. 2C, 6F). In older cormidia, new palpon cluster formation was inferred at the anterior end of each cormidium (Fig. 8A) based on differences in the sizes of palpons. The individual palpon clusters were clearly separated from each other on the siphosomal stem (Fig. 8A) even though this separation was not obvious when the specimen was observed macroscopically. The very proximal part of the palpacle was tinged orange, while distally it was a translucent white (Fig. 8A–D). Particularly in fixed material a ring-like basigaster region of the palpon became obvious just distal to the palpacle attachment point (Fig. 8C). Developing nematocysts were discerned in this region. Proximally, nematocysts were densely packed on one side of the palpacle, but more distally they were separated into pairs and continued as such along the remainder of its length (Fig. 8D).

Gastrozooids: The maximum length of fixed gastrozooids was 18 mm. The peduncles of the mature gastrozooids were short, translucent and did not bear other zooids (Fig. 8E). The proximal portion of the gastrozooid was deep red in live animals (Fig. 8E). Gastrozooids had a ring-like basigaster just distal to the peduncle, where developing nematocysts were found. The distal end of the gastrozooid was milky-white. Stripes were visible in many cases, which were reflected by ectodermal grooves in the distal parts of the gastrozooids (Fig. 8E). The diminutive gastrozooid tentacles were not conspicuous in macroscopic images, and were only apparent in fixed gastrozooids that were separated from the stem (Fig. 8F). As in other apolemiids, they bore no tentilla.

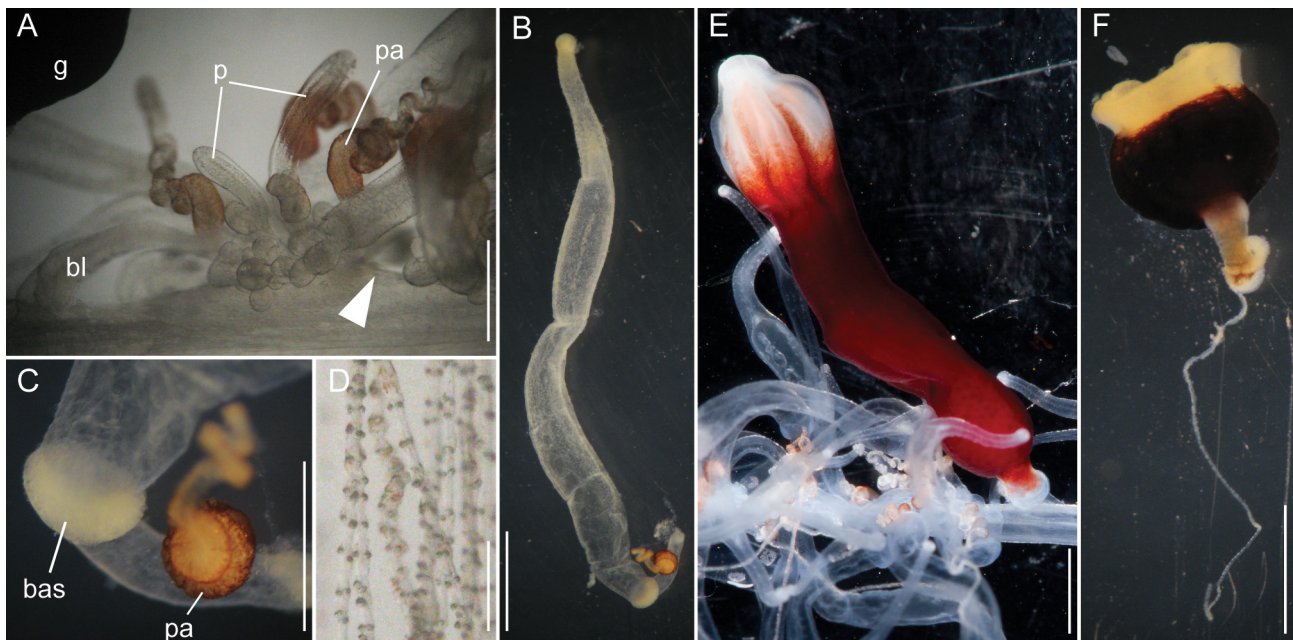


FIGURE 8. *Apolemia lanosa* sp. nov. Palpons and gastrozooids. (A) The most anterior palpon cluster of a cormidium. The arrow indicates bare stem in between youngest palpon clusters and the next older cluster. Scale bar 1 mm. (B) Mature palpon. Scale bar 2 mm. (C) Close-up of proximal end of palpon in B showing basigaster and the proximal end of palpacle. Scale bar 1 mm. (D) Distal regions of palpacles with pairs of nematocysts. Scale bar 200 μ m. (E) Gastrozooid of the holotype (live). Scale bar 2 mm. (F) Gastrozooid of specimen D329-SS6 with tentacle. Scale bar 2 mm. A, E holotype (living). B, C, F specimen D329-SS6 (fixed).

Gonodendra: Female gonophores were found along the siphosomal stem of specimen D423-D12 (Fig. 9). Gonodendra inserted directly on the siphosomal stem laterally to palpon clusters. There were several gonophores in different stages of maturation per gonodendron. Each gonophore was attached to the stalk of the gonodendron via a peduncle (Fig. 9B). The stalks of the gonodendra were small and inconspicuous. Each gonophore contained a single egg.

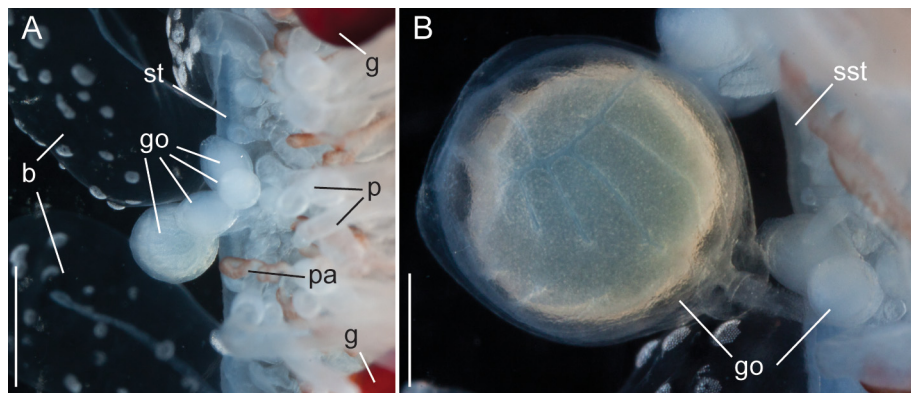


FIGURE 9. *Apolemia lanosa* sp. nov. Female gonophores (live). (A) Ventral view of palpon clusters framed by two gastrozooids (g). A cluster of female gonophores (go) is attached laterally. Scale bar 2 mm. (B) Close-up of a single female gonophore. Two smaller gonophores can be seen to the right. Gonophores sit on peduncles which attach to the stalk of the gonodendron (not visible) which itself is a small protrusion on the stem of the colony. Scale bar 1 mm.

Nematocyst complement: Four types of nematocysts were documented across the different zooids of the colony (Fig. 10). These were:

a) Spherical isorhizas of two distinct sizes.

Macroisorhizas, with a mean diameter of 22.2 μ m (Fig. 10A). The evaginated tubule was isodiametric and holotrichous. These nematocysts formed the patches on nectophores and bracts. Spherical refractile spots (mean

diameter 47.2 μm , n=12) present in between and within patches were cellular, as indicated by the presence of nuclei (Fig. 9A).

Microisorhizas, 7.2 μm (mean) in diameter (Fig. 10E,H) that were found at the distal ends of gastrozooids, palpons and nectophoral palpons, and were scattered along the body columns of these zooids in lower numbers.

b) *Stenoteles*, with a mean length of 17.9 μm and a mean width of 13.7 μm (Fig. 10B,E,G). These were found in the same locations as the microisorhizas and were highly abundant at the distal ends of the three types of zooid.

c) *Microbasic mastigophores* (Fig. 10C,E) could be found at the tips of gastrozooids, palpons and nectophoral palpons with densities being highest on gastrozooids and palpons. They were elongate (mean length 57.8 μm , mean width 21.9 μm) and slightly banana-shaped.

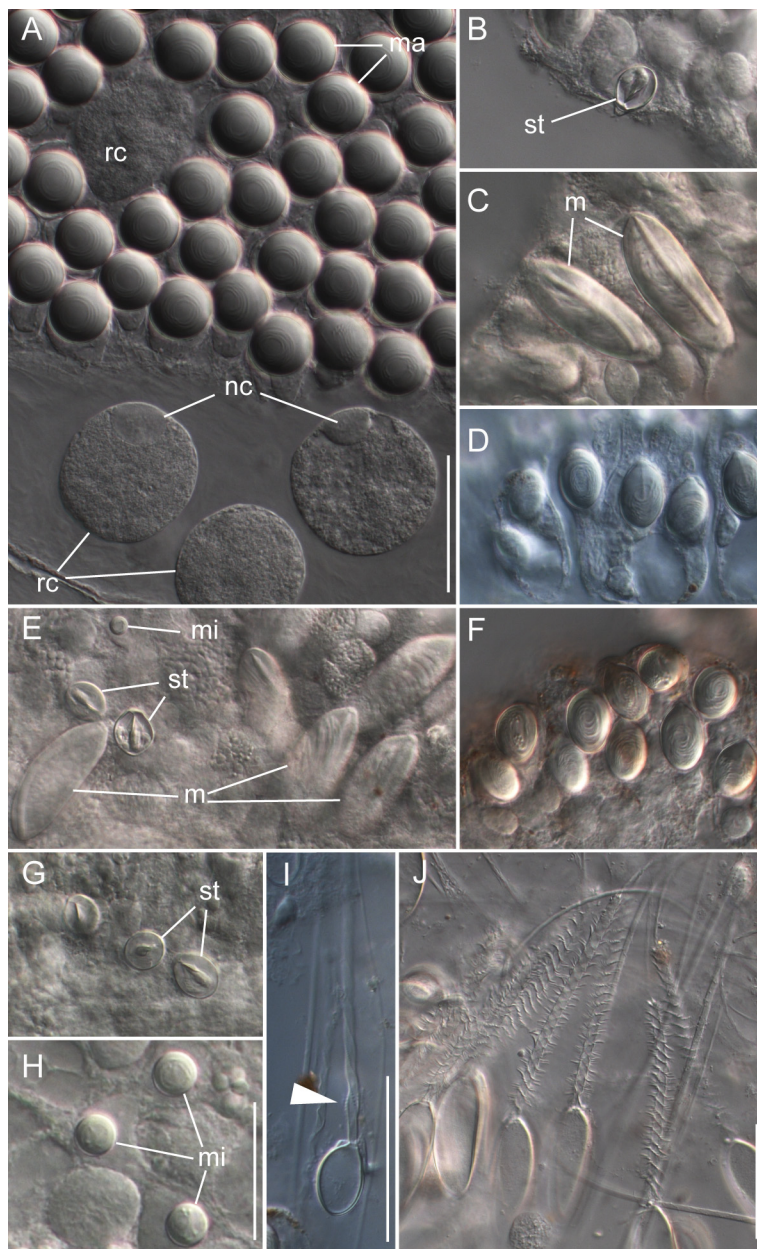


FIGURE 10. *Apolemia lanosa* sp. nov. Nematocyst complement of the holotype. (A) Nematocyst patch of macroisorhizas on the upper surface of a nectophore. Refractile elements on nectophores and bracts were cellular as indicated by the presence of nuclei. (B) Stenoteles at the distal end of a gastrozooid. (C) Microbasic mastigophores at the distal end of a gastrozooid. (D) Ovoid capsules of the gastrozooidal tentacle. (E) Stenoteles and microbasic mastigophores at the distal ends of palpons. (F) Ovoid capsules of a palpacle, apparently identical to those on the gastrozooid tentacles. (G) Stenoteles at the distal end of a nectophoral palpon. (H) Microisorhizas at the distal tip of a nectophoral palpon. Scale bar 25 μm . (I) Discharged capsule from a palpacle. Arrow indicates a single dilation on the tubule. (J) Discharged microbasic mastigophores. Scale in I, J is 50 μm . Scale bar in A (50 μm) applies to A–G.

d) The capsules of tentacles and palpacles were ovoid in shape with a mean length of 22 µm and a mean width of 14.6 µm (Fig. 10I). They were found on the palpacles and gastrozooidal tentacles. The evaginated tubule was isodiametric and holotrichous with a single dilation at the end of the shaft close to the distal end of the capsule. This was in contrast to the two dilations in birhopaloids as described for *Apolemia uvaria* (Claus 1863; Totton 1965).

Distribution. The holotype and paratype specimens, described above, both came from the vicinity of Monterey Bay, California. Several other specimens from the same region have either been collected or identified from *in situ* photographs, as listed in Table 1. The mean depth for all these specimens is 1193 ± 285.7 m. The species has also been pictured in Burton and Lundsten (2008) at the Davidson Seamount over a depth range 439–1159 m. Photographic material strongly suggests that *A. lanosa* has been collected off Japan (Lindsay 2005, 2006). The probability that there are further records is discussed below.

Etymology. The specific name *lanosa*, derived from the Latin *lana*, meaning woolly, refers to the fleece-like appearance of the siphosome of the living colony.

TABLE 1. Specimens of *Apolemia lanosa* sp. nov. observed or collected in the vicinity of Monterey Bay, California, by ROVs *Tiburon* (T) and *Doc Ricketts* (D).

Vehicle dive	Date	Location	Depth (m)	Observation type
T238	15 th November 2000	36.5842°N, 122.515°W	1070	collected in suction sampler
T260	27 th February 2001	36.5699°N, 122.5194°W	1812	frame grabs/pictures
T363	2 nd October 2001	36.5740°N, 122.5201°W	1162	frame grabs/pictures
T364	2 nd October 2001	36.3364°N, 122.8998°W	1138	frame grabs/pictures
T395	20 th February 2002	36.3295°N, 122.9011°W	928	frame grabs/pictures
T435	11 th June 2002	36.7084°N, 122.0555°W	1200	frame grabs/pictures
T438	12 th June 2002	36.5803°N, 122.4923°W	1197	frame grabs/pictures
T480	24 th September 2002	36.5770°N, 122.5241°W	767	frame grabs/pictures
T531	13 th March 2003	24.3168°N, 109.2003°W	1179	frame grabs/pictures
T596-D5	19 th July 2003	36.6021°N, 122.3746°W	1155	collected
T650	30 th January 2004	36.3296°N, 122.8976°W	1047	frame grabs/pictures
T683	5 th June 2004	36.6970°N, 122.0483°W	1070	frame grabs/pictures
T744-D1	5 th October 2004	35.4962°N, 123.8670°W	1506	collected, various pictures
T765	19 th November 2004	36°34.34'N, 122°31.3'W	1255	frame grabs/pictures
T835	23 rd March 2005	36.3231°N, 122.9141°W	1153	frame grabs/pictures
T1110-SS2/1	1 st August 2007	34.3833°N, 122.0007°W	1260	collected
D327-D4	4 th December 2011	35°56'N, 122°55'W	636	Holotype specimen
D329-SS6	6 th December 2011	36°6.99'N, 122°54.01'W	1030	Paratype specimen
D423-D12	2 nd October 2012	36°15.02'N, 122°9.98'W	1325	Paratype specimen

Apolemia rubriversa sp. nov.

Material examined: *Doc Ricketts* Dive D331-D4, 07 Dec 2011, 36°41.99'N, 122° 5.99'W, depth 650m.

Doc Ricketts Dive D195-D5, 07 Oct 2010, 36° 35.97'N, 122° 8.928'W, depth 780m.

Ventana Dive V908, 20 June 1995, 36° 42.34'N, 122° 02.24'W, depth 609m.

Only the anterior parts of the colonies, including the pneumatophore, nectosome, and anterior siphosome were collected. *In situ* high-definition videos were recorded for both *Doc Ricketts* specimens (Supplementary video, for *Doc Ricketts* D311-D4 specimen). The following observations were made on the holotype and on live tissue if not stated otherwise.

Holotype: The specimen from *Doc Ricketts* dive D311-D4 has been designated as the holotype. The specimens from *Doc Ricketts* dive D195-D5 and *Ventana* Dive V908 have been designated as paratypes. All three specimens have been deposited at the National Museum of Natural History, Smithsonian Institution, Washington DC (USNM 1207947, USNM 1207948 and USNM 1207949, respectively).

Diagnosis. Nectophores, with upper and upper lateral surfaces densely covered in patches of nematocysts. Refractile cells sparsely scattered between, but not within, these patches. Lateral radial canals with up to three distinctive diverticula extending along the wall of the nectosac and not penetrating into the mesoglea. Two median patches of red pigmentation present on the lower surface; one in the vicinity of the thrust block and the other, more prominent, one in the ventral groove.

Siphosomal growth zone with pronounced horn. Cormidia pedunculate. All siphosomal zooids borne on the peduncle of the gastrozooid, with naked stem between them. The cormidia with distinct biserial arrangement and peduncles attach left and right from the midline. Upper surface of bract entirely covered with patches of nematocysts, with refractile cells present outside of nematocyst patches predominately at the margins of the upper bract surface. Bracteal canal usually with distinct diverticula penetrating into the mesoglea. One type of palpon.

General appearance: The overall appearance of the colony was brown-red in color. This was mainly caused by colored gastrovascular fluid within the gastric system (Fig. 2B,D). The bracts were nearly transparent and gave the siphosome a ragged appearance rather than a well-defined outline (Fig. 2B,D).

Pneumatophore: The pneumatophore of the holotype was oval, approximately 3.3 mm in height and 1.7 mm as maximum diameter (Fig. 11A). The gas-filled pneumatostaccus was covered with orange pigment.

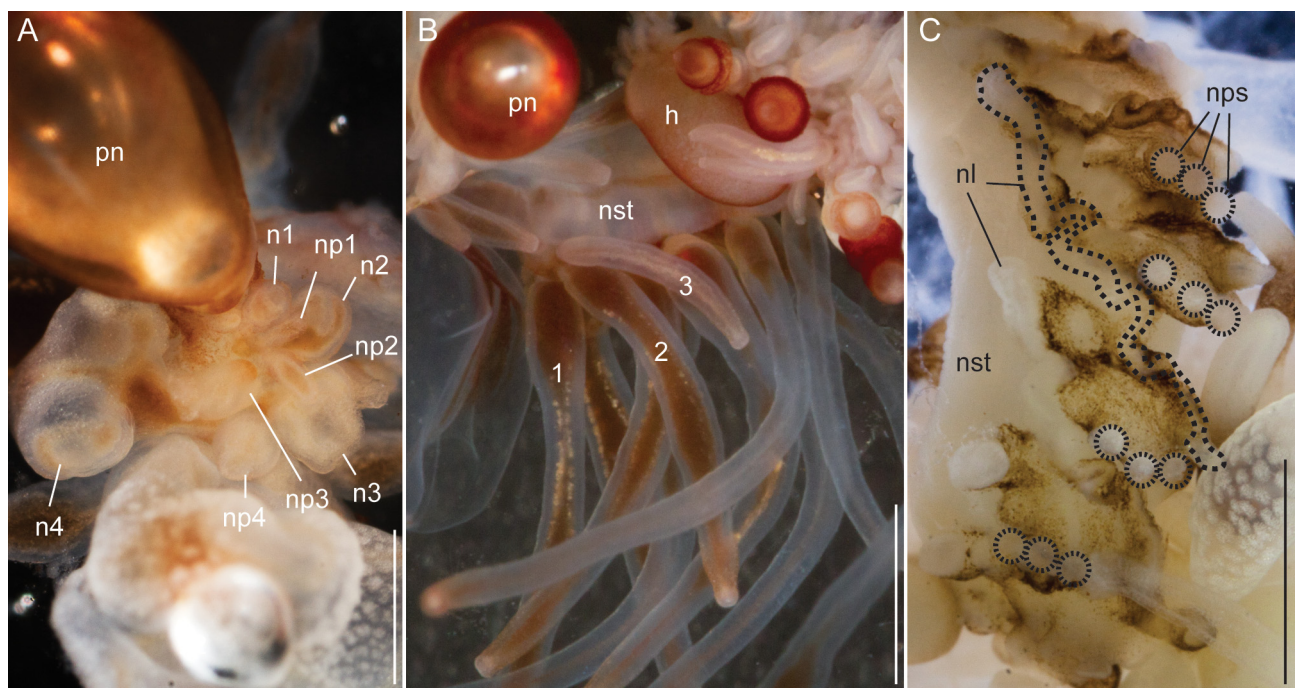


FIGURE 11. *Apolemia rubriversa* sp. nov. Nectosome of the holotype (live, A,B) and specimen D195 (fixed, C). (A) Nectosomal growth zone and pneumatophore. Older nectophores, densely covered in nematocysts, are at the bottom of the frame. Anterior is pointing out of the page, ventral to the lower right of the pane. (B) Contracted nectosome and anterior portion of the siphosome. Anterior is to the left, ventral is down. 1, 2, 3: nectophoral palpons accompanying a single nectophore. Nectosomal palpons with colored gastric content. Scale bar 2 mm. (C) Ventral view of posterior part of the nectosome showing nectophoral palpon attachment scars (dashed circles) to the left of the posterior end of the associated nectophore lamellae. Dashed line indicates one nectophore lamella. Scale bar 2 mm.

Nectosome: All but one of the mature nectophores of the holotype specimen became detached from the nectosome during the sampling procedure (Fig. 11B) but were retained in the sampler. The youngest nectophores were each accompanied by a single palpon (Fig. 11A). The nectophores were attached to the ventral side of the stem, i.e. on the same side that the siphosomal zooids were attached. Up to three palpons were associated with a single mature nectophore for the holotype and specimen D195 (Fig. 11B,C). The palpons in the nectosome were translucent white, and were up to two times the length of associated nectophores in relaxed state. The nectophoral

palpons were attached to a protruding tissue fold at the posterior end and, in ventral view, left of the nectophoral lamella (Fig. 11C).

Nectophores: In the growth zone, the more developed nectophores were densely covered with opaque nematocysts (Fig. 11A). In older nectophores these nematocysts were organized in distinct patches. The largest nectophore of the holotype had a length of 14 mm, and a width of 10 mm. Mature nectophores had large axial wings (Fig. 12). Whereas immature nectophores were widest at mid-height of the nectophore, mature ones were widest at the apical tips of the axial wings (Fig. 12A,N). Patches of nematocysts covered the upper and upper-most lateral surfaces, including the axial wings (Fig. 12). There were no lateral nematocyst patches below the lateral furrows. Refractile cells were sparsely scattered between but not within these patches of nematocysts.

Deep lateral grooves approached the upper side at approximately half the length of the nectophore, which resulted in indentations in the sides of the nectosac. On the upper side of live nectophores these grooves ran slightly in the ostial direction before they met in the mid-line (Fig. 12A,D). In fixed nectophores, however, the grooves were even more pronounced (Fig. 12G–N). On the upper side close to the midline they bent through almost 90° to turn in the ostial direction and ran around the axial wing margins before turning toward the mid-line and uniting with the opposite groove. Laterally the grooves continued along the lower lateral sides of the nectophore and ended below the ostium (Fig. 12F).

Nectophores had a wide ostium, and the nectosac was broad at the distal end of the nectophore, occupying most of its width. Slightly proximal to this region, the nectosac narrowed considerably, before expanding in width just before the lateral furrow. The nectosac was indented by the lateral furrows and expanded again to reach its maximum or equivalent width proximal to the lateral grooves (Fig. 12).

In lower view, the inner margin of the axial wings of the nectophore gradually curved toward the mid line and tapered out well apart from each other before reaching the mid-length of the nectophore (Fig. 12B,E). Some red pigmentation was present in the region of the thrust block (Fig. 12B). The outer wing margins curved inwards at about the mid-length of the nectophore and met below the ostium. On the lower side of the nectophores the mesoglea formed pillows on either side of the median lower furrow. Where the furrow was deepest and narrowst, red pigmentation was present on its walls (Fig. 12B). In living nectophores the distal part of the lower surface only slightly protruded below the ostium (Fig. 12A,D). In fixed nectophores this protrusion was very pronounced (Fig. 12J–N). This suggests a stabilizing or antagonistic function of the lower mesoglea pillows flanking the lower furrow. This structural element seems to be less affected by the fixation procedure, whereas other parts of the nectophore might have a greater tendency to shrink, causing the differences in appearance between fixed and living nectophores.

The ascending pallial canal arose from the pedicular canal at about 1/4 the height of the nectosac and then ran toward the upper surface for a short distance to end half way up the thrust block (Fig. 12F). The pedicular canal also gave rise to the upper and lower radial canals. The upper radial canal was fairly straight on the upper surface. Just distal to where the lateral furrows joined, the canal widened slightly, kept a larger diameter and ran down to the ostial ring canal (Fig. 12D). Within the region where the lateral furrows joined small protuberances could be observed occasionally on the irregular wall of the upper radial canal.

The lateral radial canals arose at the same level from the upper radial canal at mid-height of the nectosac (Fig. 12F). They ran away from the midline and slightly up to reach the sides of the nectosac just above its widest point. In mature nectophores, in this region the lateral radial canals had up to three distinct diverticula. The outermost, on the proximal-lateral margin, was the longest and pointed towards the ostium (Fig. 12E,F). The other two were shorter, if present at all, with the one closest to the junction of the lateral canals ascending and the next descending. Presence or absence of diverticula was not a solely function of ontogenetic stage. In the holotype specimen, medium-size nectophores could be found without a single diverticulum whereas diverticula were clearly present in smaller and larger nectophores. At the position where the outermost diverticulum branched off, the lateral radial canal turned upwards and curved over onto the upper surface of the nectosac and eventually, in a slightly undulating manner, down. The canal either descended along the base of the lateral furrow, or more usually crossed that furrow and then began to descend parallel with it (Fig. 12F). Before reaching the lower margin of the nectosac the canal then curved upwards and ran obliquely to join the ostial ring canal (Fig. 12F).

In specimen V908, only one mature nectophore was available. It had all three characteristic diverticula (not shown).

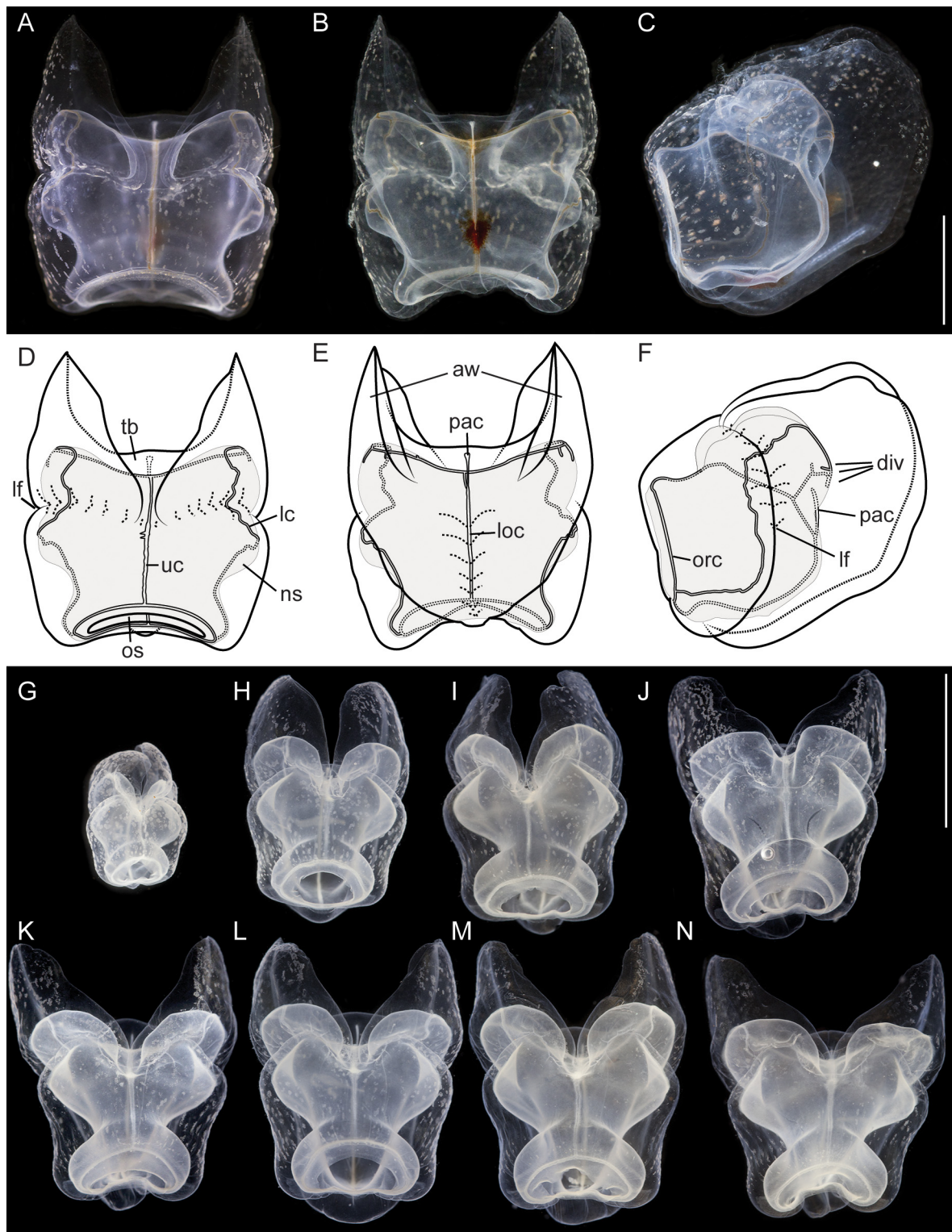


FIGURE 12. *Apolemia rubriversa* sp. nov. (A–F) Medium sized nectophore of the holotype (live). Canals were colored red by prey pigment. Photographs and drawings of upper (A, D), lower (B, E) and lateral (C, F) views. Lower view of type specimen (B) revealed red pigmentation within the ventral furrow and on the thrust block. Scale bar (5mm) in C applies to all figures A–F. (G–N) Available fixed nectophores of sample D195 shown in upper view. Scale bar (1 cm) in J applies to G–N.

Siphosome: The full length of the siphosome of the holotype prior to collection was about 1.2m in the state of relaxation as pictured in Fig. 2B. After relaxation, the siphosome of the partial holotype fragment that was collected measured 1.8 cm in length (Fig. 2D).

Siphosomal growth zone and early zooid organization. The siphosomal growth zone of the holotype had a

massive horn that bent, in ventral view, to the left side of the colony (Fig. 13). The horn was covered with a thin layer of orange-red pigment, which was easily detached when the horn was manipulated (Fig. 13B,C). The anterior end of the horn was free of zooids (Fig. 13C). The first observable buds became gastrozooids, which were alternately displaced to the left and right off the ventral midline resulting in a pronounced biserial organization (Fig. 13A, B). Additional buds became visible on the peduncle of the fourth-youngest gastrozooid (Fig. 13B). At the distal end of the peduncle, the diameter of the developing gastrozooid widened and its body had a cone-shaped appearance (gastrozooids 3–7, Fig. 13B). Just distal to the base of the cone, a constriction became apparent in gastrozooid 6 which generated a ring-like structure (gastrozooid 7, Fig. 13B). The opaque appearance of this structure indicated a site of nematogenesis and thereby the formation of the basigaster region. By gastrozooid 9, it was obvious that the buds on the peduncle of the gastrozooid gave rise to palpons. No tentacle formation could be observed in early gastrozooids.

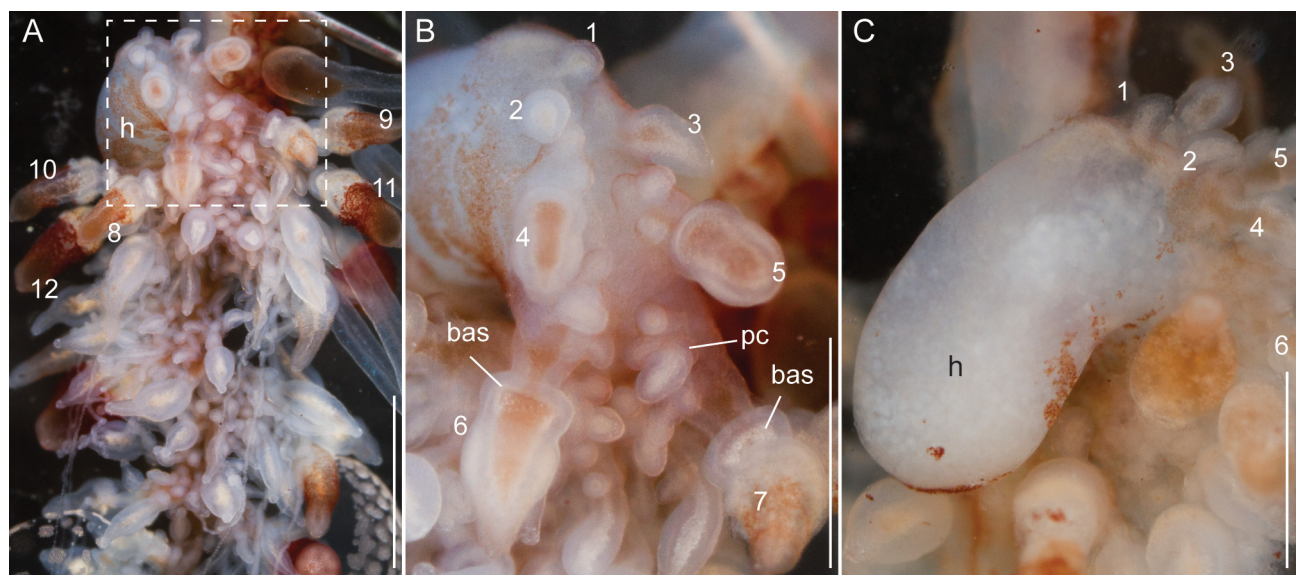


FIGURE 13. *Apolemia rubriversa* sp. nov. Early siphosomal organization of the holotype (live). Ventral view, anterior up. Numbers indicate gastrozooids starting with the youngest. (A) Anterior part of the siphosome. Frame indicates region shown in B. (B) Close-up of siphosomal growth zone. Gastrozooids (numbered) become arranged in a defined biserial organization. Palpon buds are first visible at the base of the gastrozooid and later on the gastrozooidal stalk. An indentation forms at the proximal end of the gastrozooid body separating the future basigaster region from the main body. Nematocysts become visible as opaque cells in basigaster of gastrozooid 7. (C) Siphosomal horn bending towards the right side of the siphosomal stem. Pigment has been lost as a result of tissue manipulation. Scale bars in (A) 2 mm, (B, C) 1 mm.

Bracts: Bracts were mottled with irregular shaped patches of nematocysts distributed across their upper surface (Fig. 14). These patches formed early in bract development and the distance between them increased as the bracts matured (Fig. 14A). Refractile cells were scattered sparsely and predominantly on the periphery of the upper surface outside of the opaque nematocyst patches (Fig. 14B,C). The bracteal canal ran close to lower surface throughout its length. At the distal end, however, it bent into the mesoglea (Fig. 14D). The wall of the bracteal canal in young bracts was irregularly shaped, giving it a rough appearance (Fig. 14B). Older bracts frequently, but not always, had diverticula penetrating into the mesoglea (Fig. 14D). Mature bracts had a distinct keel (Fig. 14E). Bracts were associated either with a palpon or a gastrozooid (see below). We found no morphological differences between the bracts attached at these different locations.

Palpons and gastrozooids: The body column of gastrozooids was colored by a deep red pigment. This pigment gradually faded out close to the distal end so that the oral region was white. Multiple clusters of zooids were attached to the gastrozooid peduncle (Fig. 15A). At the base of each gastrozooid peduncle a single curled lamella frequently could be observed, indicating the point of attachment of a single gastrozooidal bract (Fig. 15A). The secondary branches themselves were branched. Palpons sat on and budded off these secondary branches. Each palpon had a palpacle and was accompanied by a bract. Mature palpons were translucent with a distinct white tip. The palpacle originated at the very base of the palpon (Fig. 15B). A distinct basigaster region could not be observed. In the holotype, cells with red pigment were visible in live or freshly fixed tissue in the distal region

where the obvious gastric cavity ended, and the proboscis region began (Fig. 15C). A region with very large cells could be frequently observed along one side of the palpons (Fig. 15B,C). Tentacles associated with gastrozooids could be found in fixed tissue, but these tentacles were difficult to distinguish in live tissue (Fig. 15D).

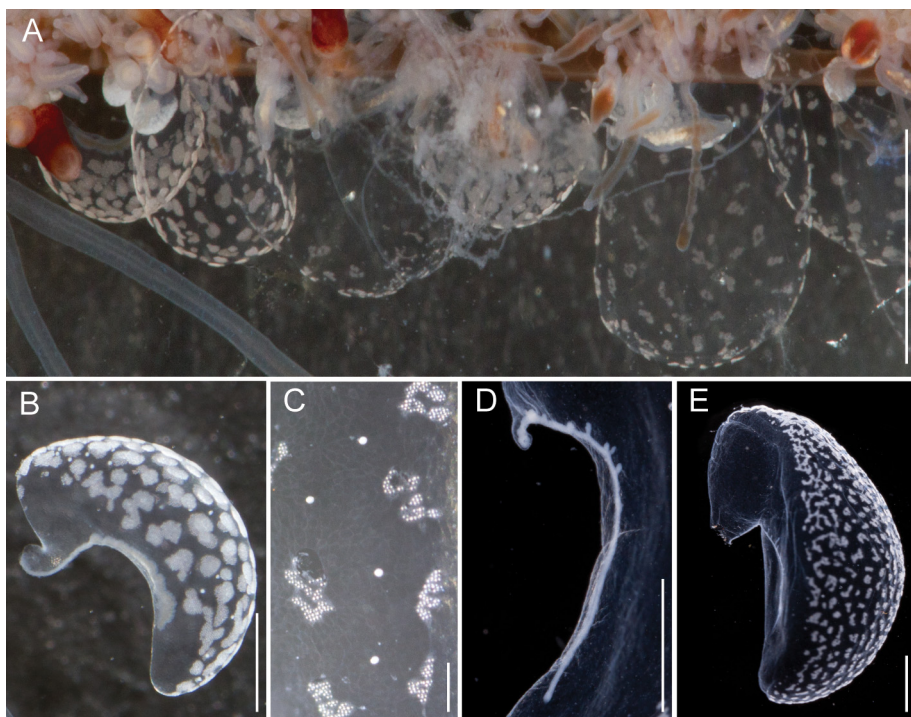


FIGURE 14. *Apolemia rubriversa* sp. nov. Bracts of the holotype (living A,B,C) and specimen D195 (fixed, D,E). (A) Change of nematocyst patch distribution during bract maturation. Anterior to the left. Scale bar 3 mm. (B) Young bract with irregularly shaped bractal canal. Scale bar 1mm. (C) Refractile cells (white dots) scattered in between but not within nematocyte patches. Scale bar 400 μ m. (D) Bractal canal with diverticula, and the distal end (at bottom) of the canal penetrating into the mesoglea. Scale 2 mm. (E) More mature bract with distinct keel. Scale bar 2 mm.

Gonodendra: Male gonodendra were found along the siphosomal stem of specimen V908 (Fig. 16). The tissue was highly contracted and detailed studies of cormidial organization could not be conducted. However, branches exclusively bearing gonophores, attached by thin peduncles, could be removed from the colony. Young palpons at the base of these branches indicated palpon bearing secondary branches as the point of their attachment (Fig. 16B).

Nematocyst complement: Four different types of nematocysts were found on the different zooids of the colony (Fig. 17).

Spherical isorhizas of two distinct sizes.

Macroisorhizas, with a mean diameter of 21.0 μ m (Fig. 17A) found exclusively in nematocyst patches on nectophores and bracts. Refractile cells were not observed within these patches.

Microisorhizas, with a mean diameter of 5.8 μ m. These nematocysts were found predominantly at the distal ends of gastrozooids, palpons and nectophoral palpons and scattered along the body columns of these zooids and in very high densities at the tip of the nectophoral palpons (Fig. 17 G,H).

b) **Stenoteles**, with a mean length of 14.1 μ m and a mean width of 11.2 μ m. These were regularly found interspersed between the macroisorhizas of the bracts and nectophores (Fig. 15A). Stenoteles were also found predominantly at the distal ends of gastrozooids, palpons and nectophoral palpons and scattered along the body columns of these zooids (Fig. 17B,E,G).

c) **Unknown type**, with a mean length of 26.7 μ m and a mean width of 16.1 μ m.

Microbasic mastigophores as described for *Apolemia lanosa* (Fig. 10C,E) were not found. The unknown capsule type was, however, found in corresponding locations at the tips of gastrozooids and palpons (Fig. 17C,E). It was smaller than the mastigophores of *A. lanosa* and was ovoid in shape. Unfortunately, no discharged capsules of this type were found.

d) **Capsules of tentacles and palpacles**, mean length 15 μ m in length and mean width 9.1 μ m (Fig. 17D,F).

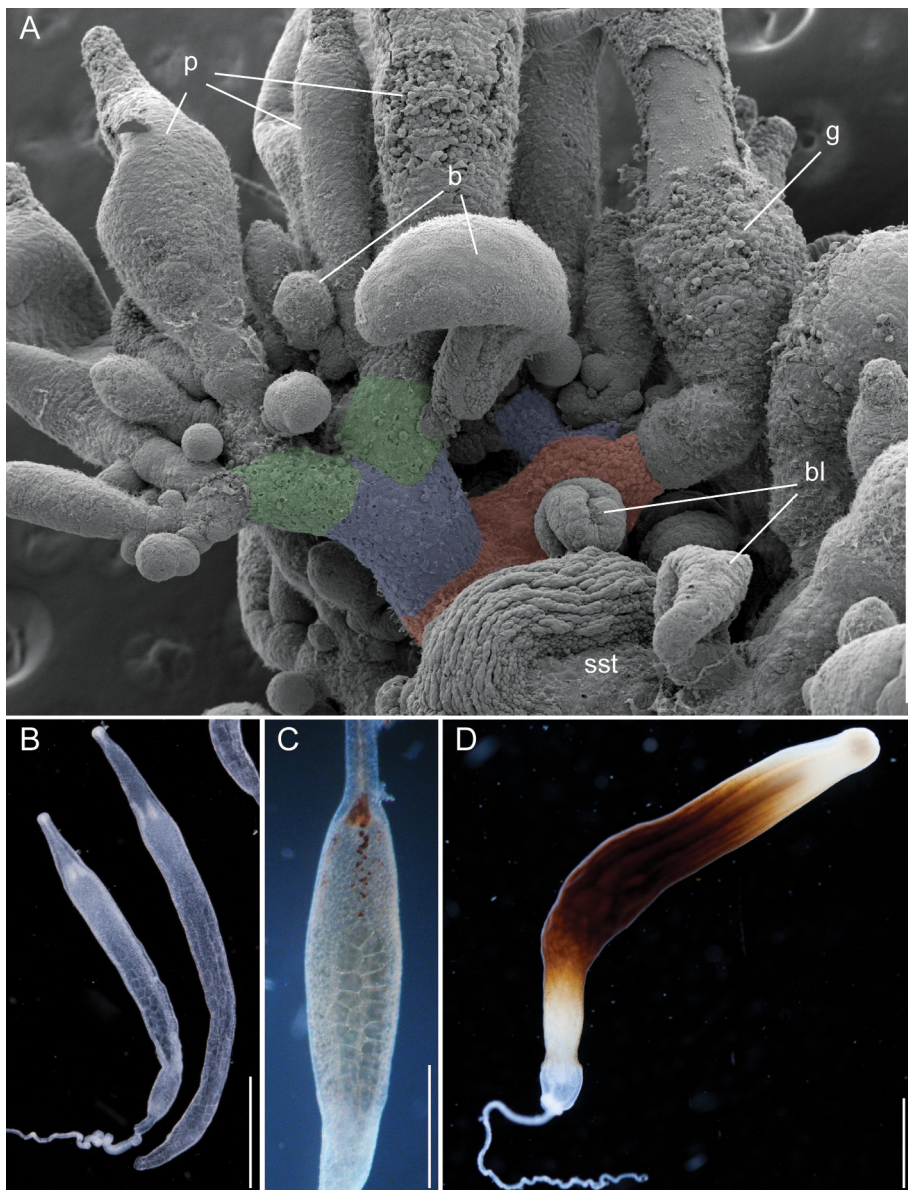


FIGURE 15. *Apolemia rubriversa* sp. nov. Palpons, gastrozooids and siphosomal organization of the holotype (A,C) and specimen D195 (B, D) (fixed tissue). (A) SEM of branched cormidium with primary branch (red) bearing the gastrozooid. Secondary branches (blue) branch off the primary branch and branch further (green). Palpons bud off branches of higher order and could be found at all different stages of development. Each palpon was accompanied by a bract and a palpacle. Scale 500 µm. (B) Mature palpons. Scale 2 mm. (C) Close-up of palpon showing highly prismatic cells and red pigmented cells in the distal region where the main gastric cavity ends. Scale 1 mm. (D) Mature gastrozooid with tentacle. Scale 2 mm.

The ovoid capsules of the tentacles and palpacles were similar in appearance to the rhopaloids found on the palpacles and tentacles of *Apolemia lanosa* but, unfortunately, their true identity could not be established as no discharged capsules were found. For the palpons, the base of the palpacle was found to be a nematogenic region. No mature capsules were found there, whereas they could easily be identified more distally, but developing nematocysts were identified.

Distribution. The holotype and paratype specimens all came from the vicinity of Monterey Bay, California. Several other specimens from the same region have either been collected or identified from *in situ* photographs, as listed below in Table 2. One specimen, however, was collected at the southern end of the Gulf of California, Mexico. The mean depth for all these specimens was 649 ± 151 m. Similar morphology has been reported for nectophores collected off Vancouver Island (Mapstone 2009, p. 83, Fig. 13) and described as “*Apolemia* sp.”, raising the possibility that they are the same species. Mapstone (2009) also reported more findings of this particular

Apolemia sp. from Bahamian waters taken by manned submersibles JSL I and JSL II, which would extend the geographic distribution of *A. rubriversa* if they prove to belong to that species. There are, however, critical differences between the nectophores of these samples and those of *A. rubriversa*. The nectophores described by Mapstone (2009) did not have diverticula on the lateral canals or nematocyst patches. Thus it will be necessary to have more complete material in order to make a definitive statement about the identity of those samples.

Etymology. The specific name *rubriversa* is derived from the Latin for red furrow, indicating the red pigmentation in the lower furrow of the nectophore.

TABLE 2. Specimens of *Apolemia rubriversa* sp. nov. observed or collected in the vicinity of Monterey Bay, California.

Vehicle dive	Date	Location	Depth (m)	Observation type
V908	20 th June 1995	36° 42.34'N, 122° 02.24'W	609	Paratype specimen
V1624	18 th June 1999	36°42.70'N, 122°03.40'W	785	frame grabs/pictures
V1680-D4	27 th September 1999	36°48.14'N, 121°59.51'W	481	collected
T365	3 rd October 2001	36°33.20'N, 122°35.50'W	874	frame grabs/pictures
T411	23 rd March 2002	36°43.33'N, 122°03.88'W	374	frame grabs/pictures
T411	23 rd March 2002	36°43.33'N, 122°03.88'W	541	frame grabs/pictures
T440	14 th June 2002	36°42.04'N, 122°03.29'W	762	frame grabs/pictures
V2187	20 th June 2002	36°42.24'N, 122°03.22'W	643	frame grabs/pictures
T478	22 nd September 2002	36°42.00'N, 122°02.20'W	492	frame grabs/pictures
T512	21 st November 2002	36°19.80'N, 122°54.00'W	457	frame grabs/pictures
T543	26 th March 2003	23°37.99'N 108°47.20'W	686	frame grabs/pictures
V2187	20 th June 2002	36°42.45'N, 122°03.08'W	643	frame grabs/pictures
T673-D2	21 st May 2004	35°55.15'N 122°56.29'W	708	collected
T845	9 th April 2005	35°28.76'N 123°51.72'W	901	frame grabs/pictures
D102-D6	11th December 2009	36°04.13'N 122°17.86'W	773	collected
D141-D6	13 th April 2010	36°44.74'N, 122°06.45'W	659	collected
D152-D4	30 th April 2010	36°45.36'N 122°04.74'W	484	collected
D195-D5	8 th October 2010	36° 35.97'N, 122° 8.928'W	780	Holotype specimen
D331-D4	07 th December 2011	36°41.99'N, 122° 5.99'W	650	Paratype specimen

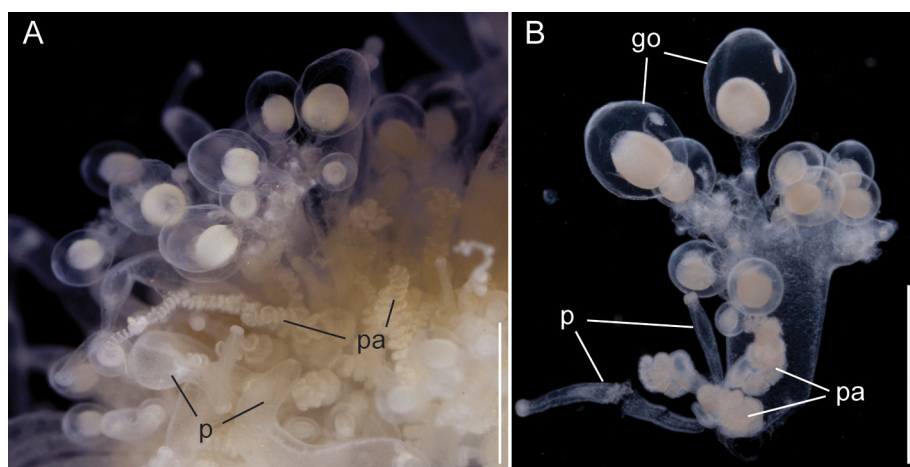


FIGURE 16. *Apolemia rubriversa* sp. nov. Gonodendra of specimen V908. (A) Gonophores protruding from palpon clusters. Scale 2 mm. (B) Gonodendron. Branch exclusively bearing gonophores with young palpons at the proximal end indicating branches with palpons as the point of attachment. Scale 2 mm.

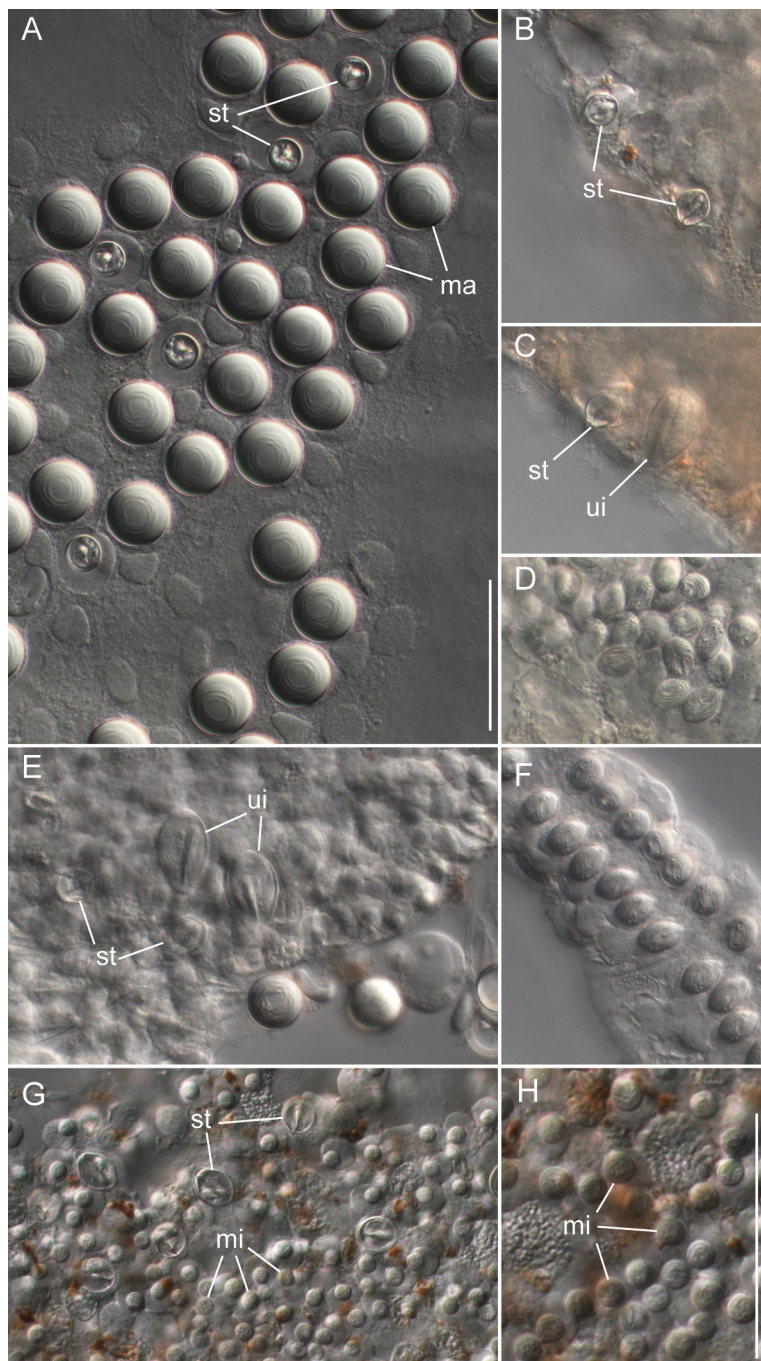


FIGURE 17. *Apolemia rubriversa* sp. nov. Nematocyst complement of the holotype. (A) Nematocyst patch on the upper bract surface. Patches on nectophores were of identical composition. Stenoteles were interspersed between spherical macroisorhizas. (B) Stenoteles from the hypostome of the gastrozooid. (C) Stenotele to the left and an unidentified capsule in the hypostomal region of the gastrozooid. (D) Ovoid capsules on the proximal part of the gastrozooidal tentacle. (E) Tip of the palpon with the unidentified capsules also seen in the hypostomal regions of gastrozooids (F) Ovoid capsules on palpacle. (G) Tip of the nectosomal palpon with stenoteles and spherical microisorhizas in very high densities. (H) Close-up of microisorhizas from the tip of the nectosomal palpons with the coiled tubule visible inside. Scale in (A) applies to (A–G) and is 50 µm. Scale in (H) is 25 µm.

Discussion

The status and diagnosis of apolemiid species. In light of the new characters introduced in the present study we re-evaluated existing literature on apolemiid species. To date, three apolemiid species have been described: *Apolemia uvaria*, *Ramosia vitiazi* and *Tottonia contorta*.

Apolemia uvaria was first figured by Lesueur (1815), as “Stéphanomie à grains de Raisin” followed by “*St. uvaria*” in the legend to the plate and “(Uviformis)” on the plate itself. As the species did not belong to the genus *Stephanomia*, Eschscholtz (1829) established the genus *Apolemia*, and referred to the species as *uvaria*. It is now a relatively well-known species (Totton 1965).

Lesueur's (1815) illustration of *Apolemia uvaria*, reproduced by Totton (1965, Plate 8) and Mapstone (2003, Fig. 14), clearly shows that there are distinct, blind ending, diverticula on the proximal parts of the lateral canals where the canals bend upwards, which protrude into the mesoglea. Unfortunately, his illustrations of the nectophores (Figs. 2–4) are upside down relative to the organismal axis; a fact noted by Totton who inverted them in his plate. Further illustrations of this arrangement are given by, for instance, Eschscholtz (1829, Pl. 13, Fig. 2), Leuckart (1854, Pl. XII, Fig. 7), Totton (1965, Fig. 14), and Mapstone (2003, Fig. 6). We were also able to document these numerous and characteristic diverticula on the lateral radial canals of the nectophore (Fig. 18A,B). According to Stepanjants (1967), *Ramosia vitiazi* also possessed diverticula on its lateral radial canals. In contrast to *A. uvaria*, these short diverticula were found along the distal, rather than proximal, loops of the lateral radial canals (Stepanjants 1967, Fig. 77). Re-examination of Stepanjants' paratype specimen revealed that these diverticula are in our opinion slight irregularities in the walls of the lateral radial canals that do not protrude into the mesoglea, and they are entirely absent in some of the paratype nectophores (see Fig. 18F–H). Thus, these structures do not appear to qualify as true diverticula.

Stepanjants believed that the siphosomal organization of *Ramosia vitiazi* differed markedly from that of *Apolemia uvaria* in that each cormidium was borne on a single stalk, which gave rise to second order branches bearing gastrozooids, more than one per cormidium and with unbranched tentacles, bracts, and palpons, with gonophores forming at the base of the palpons (Stepanjants 1967, Fig. 78). Stepanjants considered that this pedunculate arrangement was sufficient to establish a new genus for her species. Despite numerous publications on *A. uvaria*, detailed observations on cormidial organization have been rare, but a remarkable description was given by Leuckart (1854). He observed that each cormidial group was, indeed, borne on a separate stalk-like extension from the stem, i.e. it was pedunculate. Gastrozooids were found to be surrounded by a large number of palpons, and a bunch of 10–12 bracts could be found distally. It is, however, unclear if Leuckart observed more than one gastrozooid per cormidium. Lesueur's (1815) plate shows the cormidia to be separated from each other by stretches of naked stem. We were able to confirm these observations (Fig. 18C–E). Gastrozooids were located at the posterior end of short and massive peduncles (Fig. 18D) and palpons were inserted anteriorly (Fig. 18E). This arrangement was already obvious in the growth zone, which had very small and inconspicuous horn (Fig. 18C). Our findings suggest that there is a single gastrozooid per cormidium in *A. uvaria* (Fig. 18C,E). Unfortunately, all the bracts of Totton's specimen were detached, so we could not assess their distribution.

It seems likely that Stepanjants was unaware of Leuckart's description, which would have obviated the need to establish a new genus for the species *vitiazi*. This is fortunate as the generic name *Ramosia* is preoccupied by a genus of clear-winged moths (Engelhardt 1946). We therefore refer to this species as *Apolemia vitiazi*.

To date, all descriptions of *Tottonia contorta* are somewhat problematic. The original description (Margulis 1976) was based on several nectophores and a piece of largely denuded stem that included only the pneumatophore, nectosome and anterior part of the siphosome. It was collected in the Indian Ocean, midway between Sri Lanka and the Andaman Islands. Three nectophoral buds and a well-developed nectophore were attached to the stem. Margulis first included the species in Agalmatidae. Later, she (1980) re-described the species as an apolemiid, but based on two additional specimens collected in the equatorial Pacific Ocean west of the Galápagos Islands. One specimen consisted of a denuded stem, including a two-chambered pneumatophore (most likely a sampling artifact, as gas-filled pneumatophores tend to rupture when specimens are brought up the surface), a single attached and two detached nectophores, and several siphosomal zooids. This was designated the paratype. The second new specimen consisted only of siphosomal fragments. Margulis noted the presence of palpons on the nectosome of the paratype, but was unable to establish their exact distribution. She only briefly referred to the nectophores of the paratype, stating that they were identical to those of the holotype. However, the two nectophores she illustrated (Margulis 1980, Fig. 1A,B)—the attached one and a detached one—bear no resemblance

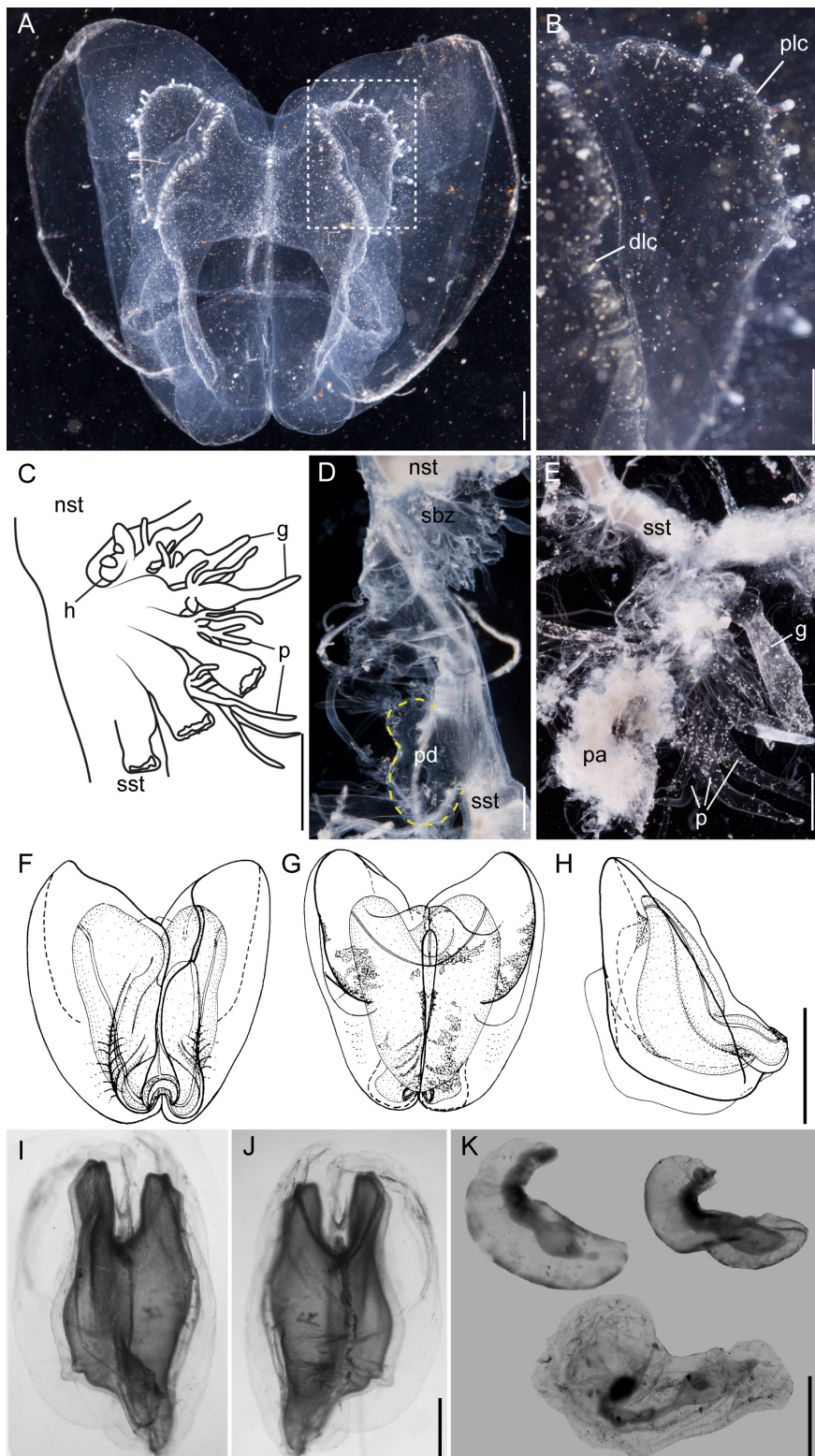


FIGURE 18. Characters of previously described *Apolemia* species. *Apolemia uvaria* (A–E). (A) Mature ectophore, upper view. Scale bar 2 mm. (B) Close-up of region highlighted in (A). Proximal loop of lateral canal with diverticula penetrating into the mesoglea. Scale bar 1 mm. (C) Siphosomal budding zone with very small horn and palpons budding from gastrozooid peduncles. Anterior is at the top. Scale bar 1 mm. (D) Anterior part of the siphosome with siphosomal budding zone. Dashed line indicates large peduncle. Zooids had been mostly detached. Anterior is at the top. Scale bar 1 mm. (E) Older cormidium with gastrozooid and palpon cluster. Tangled palpacles (pa) visible at the lower left. Anterior is to the left. Scale bar 2 mm. *Apolemia vitiazzi* (F–H). Upper (F), lower (G) and lateral (H) views of a ectophore from the paratype specimen. Scale bar 5 mm. *Apolemia contorta* (I–K). Upper (I) and lower (J) views of a ectophore from the type specimen. Scale bar 1 mm. (K) Three bracts from the paratype specimen. Scale bar 1 mm.

to each other, and only the latter vaguely resembles that of the holotype. It is therefore difficult to assess if the holotype and the paratype are of the same species.

We were able to re-examine a nectophore from the type specimen of *Tottonia contorta*, and most of the paratype specimen, which unfortunately did not include the nectophores. The nectophore of the type specimen had a very characteristic shape (Fig. 18I,J), although its ostial region had become distorted. The siphosomal zooids of the paratype specimen were definitely apolemiid and included some female gonophores. However, Margulis (1980) considered that both male and female gonophores were present on the non-paratype specimen. The latter observation was surprising to us since all specimens we have been able to analyze so far had gonophores of only one sex, indicating that apolemiid species are dioecious. This is consistent with the current understanding of the evolution of sexual systems in siphonophores (Dunn *et al.* 2005, Fig. 7), which indicates a single origin of monoecism in siphonophores after the divergence of *Apolemia*. In addition, Leuckart (1854) described *Apolemia uvaria* as being dioecious and dioecism was included in the family diagnosis (Mapstone 2009). The one very distinctive feature of the siphosomal zooids of the paratype was the structure of the bracts, although most appeared to be immature, judging by the thickness of the bracteal canal (Fig. 18K). In the largest bract the enlargement of the canal was restricted to the distal regions (Fig. 18K). In all cases the distal part of the bracteal canal bent into the mesoglea. This was consistent with the drawings provided by Margulis (1980, Fig. 1H).

Mapstone (2003) gave a further description of *Tottonia contorta*, based on three net-collected specimens from off Point Conception, California, which were collected at 1400, 400–100, and 1500 m depth. The nectophores of her samples were of relatively large size in comparison to the holotype specimen, which she was also able to examine. She commented on this fact that the holotype nectophores might be immature. To us, however, the differences do not seem to be ontogenetic, particularly as the lateral radial canals, as depicted in Margulis (1976) are not thickened, as is usually the case for young nectophores. In addition to the size differences, the length:width ratios of the nectophores were very different (see Table 3). The presence of obvious nematocyst patches on both the nectophores and bracts of Mapstone's specimens is at variance with Margulis' observations (1976, 1980) that they were completely absent. When compared to the paratype material, the arrangement of the bracteal canal was completely different in that in the Californian samples the distal end of the canal bends back to the lower surface (Mapstone 2003, Fig. 13D). Finally, Margulis (1980) appears to have described more than one type of palpon, while Mapstone only found one.

A comparison of the main characters of *Tottonia contorta* given by Margulis (1976, 1980), and by Mapstone (2003) and of *Apolemia lanosa* described herein are summarized in Table 3. Mapstone's (2003) specimens have many characters in common with *Apolemia lanosa*, but share few with the holotype and paratype of *T. contorta* described by Margulis (1976, 1980).

It therefore seems possible that the *Tottonia contorta* specimens described by Margulis (1976) and Margulis (1980) are different apolemiid species. In consideration of the additional detail presented here, it seems certain that the specimens that Mapstone (2003) described do not belong to the same species as any of the specimens Margulis referred to as *T. contorta*. The available data (Table 3) and the overlapping geographic distribution instead suggest that Mapstone's specimens from off Point Conception (34°50.68'N, 122°45.00'W (depth 1400m); 34°59.39'N 123°02.10'W (depth 400–100m); & 34°50.71'N, 122°55.40'W (depth 1500m) can be ascribed to *Apolemia lanosa* sp. nov. Mapstone (2009) identified other material, in the vicinity of both British Columbia and the Bahamas that she also ascribed to this same species. If these were indeed *A. lanosa* it would entail a significant range expansion relative to that presented here, though additional evaluation would be required to confirm these identities.

Mapstone (2009) relegated the generic names *Ramosia* and *Tottonia* to junior synonyms of the genus *Apolemia* because of the limited set of distinguishing characters available and high similarity between bract and nectophore morphology across described species. Based on the data presented herein we follow this conclusion. We think that there do not appear to be, although it is a shame to do away with a genus named after such an eminent siphonophorologist, any valid reasons to retain the generic name *Tottonia* until the characters that may distinguish different apolemiid genera have been firmly established. Consequently, we will also refer to Margulis' (1976) species as *Apolemia contorta*.

Nematocysts in Apolemia. The nematocyst complement and distribution of a cnidarian species reflects both its phylogeny and biology (Fautin 2009). In order to determine if the nematocyst complement can be of diagnostic value within *Apolemia* we studied the nematocysts of *A. lanosa* and *A. rubriversa* and compared it with the nematocyst complement of *A. uvaria* (Table 4). Carré and Carré (1973) had given a description of the nematocysts

TABLE 3. Character comparison of *Tottonia contorta* (Margulis 1967, 1980; Mapstone 2003) and *Apolemia lanosa* sp. nov. of the present study. An asterisk in the first data column indicates that observations are from Margulis (1980), otherwise they are from Margulis (1976).

	<i>Tottonia contorta</i> (Margulis 1976, 1980)	“ <i>Tottonia contorta</i> ” Mapstone (2003)	<i>Apolemia lanosa</i>
Nectophores			
Length of nectophores	Up to 8.5 mm	Up to 28 mm	Up to 21.4 mm
Length:width ratio	1.89	1.33	1.22
Patches of nematocysts	Absent	Present	Present
Refractile cells inside nematocyst patches	?	Present	Present
Diverticula on lateral radial canals	Absent	Absent	Absent
Nectosomal palpons	large, oval, with very long thin distal extensions*	enlarged proximal region and narrow distal region	enlarged proximal region and narrower distal region
Number of palpons per nectophore	Not determined	1–	Up to 4, increasing posteriorly.
Bracts			
Patches of nematocysts	Absent*	Present	Present
Distal end of bracteal canal	Swollen, ? within mesoglea*	Narrow, extends slightly into mesoglea before returning to lower wall	Narrow, extends slightly into mesoglea before returning to lower wall
No. of types of siphosomal zooids (beside gastrozooids and bracts)	? 2–3*	1	1

TABLE 4. Nematocyst complements of three apolemiid species. For each measurement minimum, maximum and mean (min/max/mean) are given. The number (n) of measurements is given in brackets for each of the dimensions.

	<i>Apolemia uvaria</i> ^a	<i>Apolemia lanosa</i>	<i>Apolemia rubriversa</i>
Macrobirhopaloids. Tentacles, palpacles, & buccal regions of gastrozooids and palpons	24 x 15 µm		
Microbirhopaloids. Tentacles & Palpacles	15 x 9 µm		
Heterotrichous microbasic eurytele/ Unidentified capsule. Tentacles & Palpacles		18.9/27.3/22.0 x 12.5/ 17.1/14.6 µm (44/53)	12.8/16.1/15.0 x 8.3/9.9/ 9.1 µm ^b (17/22)
Macrostenoteles. Buccal region of gastrozooids and palpons	26 x 23 µm		
Microstenoteles. Buccal region of gastrozooids and palpons	14 x 12 µm	16.1/19.8/17.9 x 12.7/ 14.7/13.7 µm (16/26)	12.6/16.3/14.1 x 10.1/ 12.4/11.2 µm ^c (14/29)
Macroisorhizas.	15 µm in diameter ^d	21.6/22.9/22.2 µm in diameter ^e (39)	19.7/22.0/21.0 µm in diameter ^e (27)
Microisorhizas.	7.5 µm in diameter ^d	6.5/7.6/7.2 µm in diameter ^f (19)	5.0/6.7/5.8 µm in diameter ^f (29)
Mastigophores. Buccal region of gastrozooids and palpons	32.5 x 14 µm	54.2/61.6/57.8 x 18.8/ 23.5/21.9 µm (11/16)	
Unknown. Buccal region of gastrozooids and palpons			22.7/29.2/26.7 x 14.8/ 17.5/16.1 µm (16/16)

^a: Data from Carré & Carré (1973);

^b: not identifiable;

^c: Also in patches on bracts;

^d: Both types of isorhizas found on bracts and palpacles, according to Carré & Carré (1973);

^e: Found only on nectophore and bracts;

^f: Found only on gastrozooids and palpacles, particularly in the buccal regions.

of *A. uvaria*, which consisted of isorhizas, stenoteles, birhopaloids and mastigophores, with all but the last being found in two different sizes. However, later Östman (2000, Fig. 1D) illustrated p-mastigophores of two very different size classes from a specimen of *Apolemia* sp., which earlier she had referred to as “*Apolemia uvaria (?)*”, that was collected off Catalina Island, California. This locality indicates that it might not be *A. uvaria*, which we believe to have a distribution limited to the Northeast Atlantic and the Mediterranean.

Analogously to *Apolemia uvaria* we could find two sizes of isorhizas in the two new species. We have found that only macroisorhizas were present on the bracts and nectophores, while microisorhizas were limited to the gastrozooids and both siphosomal and nectosomal palpons. In *A. uvaria*, Carré and Carré (1973) found the two sizes of isorhizas to be present on the surfaces of the bracts and palpons. It remains unclear if they found the two types on each of these two zooids and also if they found them on both siphosomal palpon types present in *A. uvaria*. Carré and Carré (1973), Totton (1965) and Mapstone (2003) made no comment as to what the types of nematocyst present on the surface of the nectophores might be. However, Claus (1863) noted for *A. uvaria* globular nematocysts, 12–14 µm in diameter, with a shaftless tubule that made up the patches on the nectophores and bracts, and also the armory of the brown siphosomal palpon type. Therefore it is possible that the two types of isorhizas are co-localized in all three species, obviously with the exception of the additional palpon type only present in *A. uvaria*. Unfortunately the state of the available *A. uvaria* specimen did not allow us to assess this hypothesis.

In contrast to *Apolemia uvaria* we could only find stenoteles of one size in *A. lanosa* and *A. rubriversa*. In all three species stenoteles were mainly found in the buccal regions of the gastrozooids and palpons. In the two new species this included the nectosomal palpons, whereas those were not considered by Carré and Carré (1973). In *A. lanosa* and *A. rubriversa*, stenoteles were, in addition, also scattered all over these zooids. Remarkably, only in *A. rubriversa* were stenoteles also found within the nematocyst patches on the bracts.

Mastigophores were found co-localized with the stenoteles in the buccal regions of gastrozooids and palpons in *Apolemia uvaria* and *A. lanosa*, including the nectosomal palpons in case of the latter. Interestingly, the capsule at corresponding sites in *A. rubriversa* was of a very different morphology but could not be further characterized. While only one form of mastigophore was present in *A. uvaria* and *A. lanosa*, Östman (2000) found two in her *Apolemia* species.

In all three species, nematocysts of tentacles and palpacles were of the same type. In *Apolemia uvaria* this capsule type has been described as birhopaloid, which is characterized by having two swellings on the proximal shaft of the evaginated tubule, and they are present in this species in two sizes. These capsules were first noted by Claus (1863), first illustrated by Iwanhoff (1896, pl. 5, Fig. 26) and confirmed by Totton (1965), and the capsule was seen as unique to *Apolemia*. Margulis (1980, Fig. 2E) was able to illustrate this capsule type for *A. contorta*, although she referred to it as a microbasic eurytele. For *A. lanosa* and *A. rubriversa* we could find only capsules of one size, as did Östman (2000) in her specimen of *Apolemia* sp. In the case of *A. rubriversa* we were not able to analyze evaginated tubules of the capsules. The tubules in capsules of *A. lanosa*, however, did show only one swelling and they could therefore not be identified as birhopaloids, but tentatively as euryteles.

Werner (1965) divided euryteles into micro- and macrobasic forms, of which the one in *Apolemia lanosa* (see Fig. 9I) is clearly microbasic. He then divided the latter into homotrichous and heterotrichous forms and, judging from his figures, the latter is closer to that found in *A. lanosa*. But Werner also noted, in his Table 3, that at that time microbasic euryteles had not been found in any siphonophore species. However, subsequently, Carré (1971, 1980) has found microbasic euryteles in the larval bracts of *Halistemma rubrum* (Vogt) and *Agalma elegans* (Sars), respectively; while Carré (1969), more specifically, found heterotrichous microbasic euryteles to be present in the cnidoband of *Desmophyes villafrancae* (Carré), which is the first and only time that this type of nematocyst has been found in a calyphoran siphonophore.

In summary, there is some consistency in the nematocyst complement across the considered apolemiid species. The data suggest that different size versions of the same capsule type emerged or got lost on multiple occasions. The same capsule type on tentacles and palpacles in all three species points to the homology of both structures. More data are needed to understand the pervasiveness of birhopaloid capsules in *Apolemia*. If the presence of birhopaloids were the ancestral state in *Apolemia*, the eurytele-like capsule observed in *A. lanosa* would be derived and it would be unlikely that this capsule is homologous to euryteles in other siphonophores. On the other hand birhopaloids could be derived from a eurytele-like capsule type present in the most recent common ancestor of *A. uvaria* and *A. lanosa*. The most striking difference was the presence of an unidentified capsule type instead of mastigophores in *A. rubriversa*. The presence in corresponding regions on different zooid types suggests a common history, but again more data are needed to understand the relationship of these two capsules types.

Based on our findings for *Apolemia lanosa* and *A. uvaria* it is worth stressing that the nematocyst complement of the body columns of gastrozooid and both the nectophoral and siphosomal palpons are all virtually identical. The nematocysts present on the tentacles and siphosomal palpacles, however, are different from those of the body-columns of the zooids that bear them. This is additional evidence in support of our belief that the structures at the base of each nectophore are indeed palpacle-less palpons rather than tentacles.

The challenges of diagnostic characters for siphonophores. There are several factors that complicate the identification of good diagnostic characters in siphonophores. The descriptions made here highlight some of these difficulties.

Specimens are often incomplete due to their fragility, size, and often less than ideal modes of collection. The problem is especially pronounced for apolemiids, since they are so long that even under ideal conditions only a portion of the colony can be collected. The anterior end includes the most structures (the pneumatophore, both growth zones, the nectosome, and the young siphosome) but often lacks gonophores.

There can be variation in the structure of the same zooids within a colony. Much of this variation, especially in nectophores (Figs. 4, 12), is ontogenetic. There is, however, sometimes non-ontogenetic variation between zooids. For example, the presence or number of diverticula on lateral canals of a nectophore can vary in ways that do not relate to position and age. Analysis of subsets of the ontogenetic series of nectophores can therefore be misleading whereas the maximum number and orientation of these diverticula might however be species specific.

Fixing siphonophore tissue can obfuscate an entire set of characters. This is especially true when analyzing cormidial organization. Shrinkage and contraction can make growth zones and cormidia inaccessible to investigation. Breaking of the siphosomal stem and irregular detachment of zooids, which frequently happens, can cause problems with orientation and deciphering cormidial patterns. Fixation also alters zooid morphology. For instance, the basigaster of the palpon becomes conspicuous (Fig. 8C), whereas it is inconspicuous in live tissue. In the case of nectophores, the fixation procedure can elevate particular characters like depth of lateral furrows; introduce characters like zigzagging of canals; and the general nectophore anatomy can favor shrinkage in particular regions, which can change the *in vivo* habitus quite noticeably. In the species considered here, for example, a protruding mouth plate below the ostium is only visible in fixed material (compare Figs. 12A,K–N). The state of contraction of the nectosac at the time of fixation can cause further variation (Fig. 4T,U). Presence or absence of pigment or nematocyst patches is often difficult to evaluate in fixed material and especially in exposed regions prone to abrasion. Ideally, *in vivo* studies after relaxation of the tissue should be complemented by analysis of fixed material, but such opportunities rarely occur.

Characters of Apolemia. From the above discussion, we believe that all five species names should be referred to the genus *Apolemia* until, with the descriptions of further species, valid generic characters can be established. The new descriptions presented here clarify interpretation of characters that have been commented on by previous authors, and suggest others that will be useful for understanding the diversity of the group as additional species are described. These characters include, as partially summarized in Table 5:

The number of nectosomal palpons at the base of each nectophore. The presence of palpons within the nectosome is unique to apolemiid species, and readily distinguishes them from all other siphonophores. Despite the number of studies on *Apolemia uvaria*, few authors have actually counted the maximum number of nectosomal palpons clustered below each nectophore and numbers given vary between 3 and 6 (Leuckart 1854; Totton 1965; Mapstone 2003). Our observations of intact specimens of *A. lanosa* and *A. rubriversa* clearly indicate that the number of palpons per nectophore actually increases with the age of the nectophore. It is likely that this is also the case for other apolemiids that also have multiple palpons per nectophore. In these cases a certain number of intact specimens will be needed to identify fully grown nectosomes and maximum numbers of palpons. We, however, have preliminary data that there are apolemiid species with just one nectosomal palpon per nectophore independent of age, as was also described for *A. vitiazi* by Stepanjants (1967) and confirmed by Mapstone (2003).

The presence of diverticula on the proximal part of the nectophoral radial canals. Although *Apolemia rubriversa* usually has up to three distinct diverticula, some mature nectophores have none. Unlike the diverticula of *A. uvaria*, these diverticula do not penetrate into the mesoglea but run along the wall of the nectosac.

Whether the cormidia are dispersed, i.e. the cormidial zooids are attached individually and directly to the siphosomal stem, or whether they are pedunculate, i.e. all borne on the peduncle of the primary gastrozooid (Fig. 19).

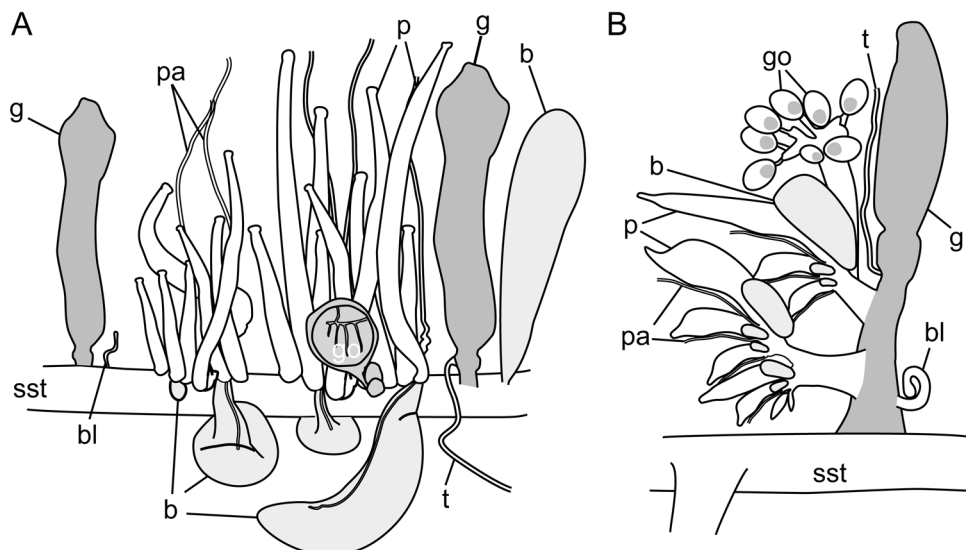


FIGURE 19. Cormidial organization of *Apolemia lanosa* (A) and *Apolemia rubriversa* (B). Anterior is to the left. Ventral is up. (A) Lateral view of the siphosomal stem showing a cormidium with two palpon clusters. The bracteal lamella (bl) of a removed gastrozooidal bract and the gastrozooid of the next younger cormidium is visible to the left. (B) Branched cormidial organization. All siphosomal zooids are attached to the stem via the gastrozooid peduncle. The proximal portion of another cormidium is shown in the lower left of the pane. Anterior is to the left. Ventral is up.

TABLE 5. Character matrix for known apolemiid species.

Character	<i>A. uvvaria</i>	<i>A. vitiazzi</i>	<i>A. contorta</i>	<i>A. lanosa</i>	<i>A. rubriversa</i>
Maximum observed number of palpons at base of each nectophore.	6	1	? 1	4	6
Presence of diverticula on lateral radial canals	Numerous, small, penetrating into mesoglea	Irregularities in thickness of walls	None	None	Up to 3, long, along nectosac
Cormidia dispersed or pedunculate	Pedunculate	Pedunculate	? dispersed	Dispersed	Pedunculate
Horn in siphosomal growth zone	Very small	Unknown	Unknown	Very small	Very large
Number of types of siphosomal palpons	2	Unknown	Unknown	1	1
Patches of nematocysts on nectophores and bracts	Present	Unknown	Unknown (Margulis 1976), Absent (Margulis 1980)	Present	Present
Refractile spheres on bracts and nectophores	Present, only outside nematocyst patches	Unknown	Unknown	Present, inside and outside nematocyst patches	Present, only outside nematocyst patches

The number of types of siphosomal palpons. To date two types of palpons have been confirmed only in *Apolemia uvvaria*, which differ in relative size, nematocyst complement and rigidity.

Whether there is a pronounced horn present in the siphosomal growth zone.

Whether patches of nematocysts are present on the surface of the nectophores and bracts.

Whether refractile spheres are present on the surface of the nectophores and bracts and whether they occur inside the nematocyst patches. This trait is likely to be affected by the condition of the specimen as nematocyst patches and refractile cells are prone to abrasion. Species of *Apolemia* are notable for their short-wavelength violet

bioluminescence (Haddock & Case 1999) originating in nectophores and bracts. Because many *Apolemia* species shed most of their bracts even when collected with ROVs, luminescence from captured specimens can appear feeble relative to that of other physonects. Cells organized in patches have been observed as the source of bioluminescence in other siphonophores (e.g., Pugh 1999; Haddock pers. obs.). In *Apolemia*, however, these patches are mainly composed of nematocysts leaving the refractile spheres as a putative source of bioluminescence.

Whether the palpons have basal palpacles; and even whether the gastrozooids bear tentacles. These structures are extremely delicate and easily lost, particularly with net collected material. At present there is insufficient evidence to suggest that this character has any taxonomic relevance with regard to the apolemiids, but it should be carefully noted in future newly-collected specimens.

The presence of a multi-chambered pneumatophore has been suggested in the past as a taxonomic character, for instance by Margulis (1980). But in life there is only one chamber, the pneumatosaccus, with the gas secreting region posterior to it, and any additional chambers are artifacts resulting from the rupture of the pneumatophore while the specimen was being brought to the surface. Thus, this feature cannot be used as a valid taxonomic character.

The available data also indicate differences in nematocyst complements across species (Table 4).

Siphosomal development and growth. Because siphonophores are fragile and are often dissociated when collected by net, the organization of zooids within the colony and the structure of cormidia in particular have largely been neglected in the discussion and description of their morphology. Recent advances in the ability to collect intact siphonophores, though, has greatly extended the ability to describe not just the structure of isolated zooids, but their organization within the colony relative to the other zooids (Dunn 2005; Dunn & Wagner 2006). This also aids in understanding the budding process that gives rise to zooids.

The work presented here clearly indicates that there are two general cormidial organizations in *Apolemia*: pedunculate and dispersed (Fig. 19). In pedunculate cormidia, all zooids of each cormidium are attached to the stem by a single peduncle, and the regions of stem between these shared peduncles are bare. In dispersed cormidia, most zooids of the cormidium are independently attached to the stem and, macroscopically, there are no portions of the stem that are devoid of zooids.

Neither of these types of organization is unique to *Apolemia*, but the fact that both are present in *Apolemia* does indicate that the evolution of cormidial organization is more complicated than had previously been thought. In Codonophora, the clade comprised of Physonectae (which is paraphyletic) and Calycophorae (which is monophyletic and nested within Physonectae), each cormidium of previously examined species arises as a single pro-bud (Dunn & Wagner 2006). This pro-bud gives rise to the primary zooids of the cormidium. The primary zooids always include a single gastrozooid, and, depending on the species, may also include bracts, palpons, and gonophores. The primary zooids of each cormidium all initially share a peduncle, which is their attachment to the stem. The pro-bud and the zooids it gives rise to, are clearly visible in *A. rubriversa* (Fig. 13B). In case of *A. lanosa* pro-buds were difficult to identify and palpons and bracts seem to arise directly from the siphosomal stem suggesting that zooid/bud dispersal happens very early in development (Fig. 5).

The subsequent development of the pro-bud varies greatly from species to species. In taxa with pedunculate cormidia, all of the zooids of each cormidium retain their shared connection to the stem. In taxa with dispersed cormidia, the primary zooids spread out along the stem as they mature and their common origin becomes obscured. All calycophorans have pedunculate cormidia (with perhaps the exception of *Stephanophyes superba* (Chun), and dispersed cormidia are widespread in “physonects”. This led Dunn and Wagner (2006) to conclude that the ancestral condition within Codonophora was dispersed cormidia, and that the pedunculate cormidia of calycophorans were the result of cormidial pedomorphy – immature juvenile pedunculate morphology was maintained throughout the growth of the cormidia.

Though pedunculate cormidia had been noted before in *Apolemia uvaria* (see the discussion above regarding the status of apolemiid species), considerable confusion and contradictions existed in the literature regarding this important point. Our confirmation of pedunculate cormidia in *A. uvaria* and the finding of this same organization in an additional species, *A. rubriversa*, clearly show that the conclusions of Dunn and Wagner (2006) were oversimplified. There has been homoplasy in pedunculate and dispersed organization across Codonophora. It may be that the most recent common ancestor of Codonophora had pedunculate cormidia, and that dispersed cormidia have arisen several times. Alternatively, this most recent common ancestor may have had dispersed cormidia, and there were multiple independent pedomorphic origins of pedunculate cormidia. Resolving these evolutionary

developmental questions will require both new observations in poorly known species as well as a more densely sampled phylogeny of siphonophores than is already available (Dunn *et al.* 2005).

Dispersal is not the only modification that can take place as cormidia mature. In many species, secondary zooids are added within each maturing cormidium. These secondary zooids often arise at precise locations relative to the primary zooids. Secondary zooids include bracts in many species, gonophores that are renewed after spawning events (Carré & Carré 1991), and the anterior-most palpons and gonophores in each mature cormidium of *Nanomia bijuga* (delle Chiaje) (Dunn & Wagner 2006). With the description here of *A. lanosa*, we can add gastrozooids to the list of secondary zooids. Furthermore, this is the first species where secondary gastrozooids have been found. Stem elongation throughout the siphosome and the origin of gastrozooids outside of the growth zone may play a role in helping some *Apolemia* species reach such great lengths. Without secondary addition of gastrozooids, all gastrozooids need to arise in the growth zones.

The origin of secondary zooids can complicate the interpretation of pedunculate and dispersed cormidia. This is because secondary zooids sometimes arise on the peduncles of other zooids. Some of the most conspicuous examples are the gastrozooid-associated palpons of *Agalma elegans* and the palpons and bracts found on the very long gastrozooid peduncles of *Forskalia* (Dunn & Wagner 2006).

All of the discussion above regarding cormidial organization pertains to Codonophora. In Cystonectae it is challenging to interpret cormidia because it is not clear that they actually have cormidia. There are reiterated sequences of zooids, but they are not derived from pro-buds that arise in a growth zone. There are two families within Cystonectae, Rhizophysidae and Physaliidae. In Rhizophysidae, whose species have elongate linear stems like most members of Codonophora, gonodendra and gastrozooids arise independently within the growth zones. *Physalia*, on the other hand, have a unique colony-level organization unlike any other siphonophore (Totton 1960). It has many branched tripartite groups, each composed of three structures. These are the feeding zooid (which has a mouth but lacks a tentacle), the ampoule (which has a tentacle but lacks a mouth), and the gonodendron (which itself has multiple zooids, including palpons and gonophores). Because there are multiple zooids per peduncle in *Physalia*, these structures can resemble the pedunculate cormidia found in Codonophora. Until more is known about their development, though, assessing their homology is not possible.

Acknowledgements

We thank Lynne Christianson and Pathikrit Bhattacharyya for their work on DNA sequencing. We also thank the MBARI crews and ROV pilots for collection of the specimens. We thank Susan von Thun for MBARI video lab support. This work was supported by an Alan T. Waterman Award from the National Science Foundation and by the David and Lucile Packard Foundation.

Literature

- Bucklin, A., Hopcroft, R.R., Kosobokova, K.N., Nigro, L.M., Ortman, B.D., Jennings, R.M. & Sweetman, C.J. (2010) DNA barcoding of Arctic Ocean holozooplankton for species identification and recognition. *Deep-Sea Research Part II*, 57, 40–48.
<http://dx.doi.org/10.1016/j.dsrr.2009.08.005>
- Burton, E.J. & Lundsten, L. (2008) *Davidson Seamount Taxonomic Guide*. Marine Sanctuaries Conservation Series ONMS-08-08. U.S. Department of Commerce, National Oceanic and Atmospheric Administration, Office of National Marine Sanctuaries, Silver Spring, Maryland, 145 pp.
- Carré, C. (1969) *Rosacea villafrancae* sp. n., un nouveau siphonophore calycophore Prayinae de la mer Méditerranée. *Beaufortia*, 16, 109–117.
- Carré, C. & Carré, D. (1973) Étude du cnidome et de la cnidogenèse chez *Apolemia uvaria* (Lesueur, 1811) (Siphonophore physonecte). *Experimental Cell Research*, 81, 237–249.
[http://dx.doi.org/10.1016/0014-4827\(73\)90130-4](http://dx.doi.org/10.1016/0014-4827(73)90130-4)
- Carré, C. & Carré, D. (1991) A complete life cycle of the calycophoran siphonophore *Muggiae kochi* (Will) in the laboratory, under different temperature conditions: ecological implications. *Philosophical Transactions of the Royal Society of London B*, 334, 27–32.
<http://dx.doi.org/10.1098/rstb.1991.0095>

- Carré, C. & Carré, D. (1995) Ordre des Siphonophores. In: D. Doumenc (ed.), *Traité de Zoologie. Anatomie, Systématique, Biologie. Tome III. Fascicule 2. Cnidaires. Cténaires*. Masson, Paris, pp. 523–596.
- Carré, D. (1971) Etude du développement d'*Halistemma rubrum* (Vogt, 1852) Siphonophore Physonecte Agalmidae. *Cahiers de Biologie Marine*, 12, 77–93.
- Carré, D. (1980) Hypothèse sur le mécanisme de l'évagination du filament urticant des cnidocystes. *European Journal of Cell Biology*, 20, 265–271.
- Claus, C. (1863) Neue Beobachtungen über die Structur und Entwicklung der Siphonophoren. *Zeitschrift für Wissenschaftliche Zoologie*, 12, 536–563.
- Colgan, D.J., Ponder, W.F. & Eggler, P.E. (2000) Gastropod evolutionary rates and phylogenetic relationships assessed using partial 28S rDNA and histone H3 sequences. *Zoologica Scripta*, 29 (1), 29–63.
<http://dx.doi.org/10.1046/j.1463-6409.2000.00021.x>
- Collins, A.G. (2002) Phylogeny of Medusozoa and the evolution of cnidarian life cycles. *Journal of Evolutionary Biology*, 15, 418–432.
<http://dx.doi.org/10.1046/j.1420-9101.2002.00403.x>
- Cunningham, C. & Buss, L. (1993) Molecular evidence for multiple episodes of paedomorphosis in the family Hydractiniidae. *Biochemical Systematics and Ecology*, 21, 57–69.
[http://dx.doi.org/10.1016/0305-1978\(93\)90009-g](http://dx.doi.org/10.1016/0305-1978(93)90009-g)
- Dunn, C.W. (2005) The complex colony-level organization of the deep-sea siphonophore *Bargmannia elongata* (Cnidaria, Hydrozoa) is directionally asymmetric and arises by the subdivision of pro-buds. *Developmental Dynamics*, 234, 835–834.
<http://dx.doi.org/10.1002/dvdy.20483>
- Dunn, C.W. & Wagner, G.P. (2006) The evolution of the colony-level development in the Siphonophora (Cnidaria: Hydrozoa). *Development Genes and Evolution*, 216, 743–754.
<http://dx.doi.org/10.1007/s00427-006-0101-8>
- Dunn, C.W., Pugh, P.R. & Haddock, S.H.D. (2005) Molecular phylogenetics of the Siphonophorae (Cnidaria), with implications for the evolution of functional specialization. *Systematic Biology*, 54, 916–935.
<http://dx.doi.org/10.1080/10635150500354837>
- Engelhardt, G.P. (1946) The North American clear-wing moths of the family Aegeriidae. *Smithsonian Institution. Bulletin of the United States National Museum*, 190, 222 pp.
- Eschscholtz, F. (1829) *System der Acalephen*. Ferdinand Dümmler, Berlin, 190 pp. + 16 Plates.
- Fautin, D.G. (2009) Structural diversity, systematics, and evolution of cnidae. *Toxicon* 54, 1054–1064.
<http://dx.doi.org/10.1016/j.toxicon.2009.02.024>
- Folmer, O., Black, M., Hoeh, W., Lutz, R. & Vrijenhoek, R. (1994) DNA primers for amplification of mitochondrial cytochrome c oxidase subunit I from diverse metazoan invertebrates. *Molecular Marine Biology and Biotechnology*, 3, 294–297.
- Haddock, S.H.D & Case, J.F. (1999) Bioluminescence spectra of shallow and deep-sea gelatinous zooplankton: ctenophores, medusae and siphonophores. *Marine Biology*, 133, 571–82.
<http://dx.doi.org/10.1007/s002270050497>
- Haddock, S.H.D. (2004) A golden age of gelata: past and future research on planktonic ctenophores and cnidarians. *Hydrobiologia*, 530/531, 549–556.
- Haddock, S.H.D., Dunn, C.W. & Pugh, P.R. (2005) A re-examination of siphonophore terminology and morphology, applied to the description of two new prayine species with remarkable bio-optical properties. *Journal of the Marine Biological Association of the United Kingdom*, 85, 695–708.
<http://dx.doi.org/10.1017/s0025315405011616>
- Iwanoff, N. (1896) Ueber den Bau, die Wirkungsweise und die Entwicklung der Nesselkapseln der Coelenteraten. *Bulletin de la Société imperiale des naturalistes de Moscou*, 10, 95–161, 323–354, Plates III–VI.
- Kölliker, A. (1853) *Die Schwimmpolyphen oder Siphonophoren von Messina*. Wilhelm Engelmann, Leipzig, 96 pp.
- Leloup, E. (1954) A propos des Siphonophores. *Volume jubilaire Victor van Straelen*, 2, 643–699.
- Lesueur, C.A. (1815) *Voyage de découvertes aux terres australes. Histoire Naturelle. Partie iconographique et gravure*. Plassan, Paris, 7 pp., 1 Table, 14 Plates.
- Leuckart, R. (1854) Zur näheren Kenntnis der Siphonophoren von Nizza. *Archiv für Naturgeschichte*, 20, 249–377.
- Lindsay, D.J. (2005) Planktonic communities below 2000m depth. *Bulletin of the Plankton Society of Japan*, 52, 113–118. [In Japanese].
- Lindsay, D.J. (2006) A checklist of midwater cnidarians and ctenophores from Sagami Bay –species sampled during submersible surveys from 1993–2004. *Bulletin of the Plankton Society of Japan*, 53, 104–110. [In Japanese].
- Mackie, G.O., Pugh, P.R. & Purcell, J.E. (1987) Siphonophore biology. *Advances in Marine Biology*, 24, 97–262.
[http://dx.doi.org/10.1016/s0065-2881\(08\)60074-7](http://dx.doi.org/10.1016/s0065-2881(08)60074-7)
- Mapstone, G.M. (2003) Redescriptions of two physonect siphonophores, *Apolemia uvaria* (Lesueur, 1815) and *Tottonia contorta* Margulis, 1976, with comments on a third species *Ramosia vitiazii* Stepanjants, 1967 (Cnidaria: Hydrozoa: Apolemiidae). *Systematics and Biodiversity*, 1, 181–212.
<http://dx.doi.org/10.1017/s1477200003001166>

- Mapstone, G.M. (2009) *Siphonophora (Cnidaria: Hydrozoa) of Canadian Pacific Waters*. National Research Council of Canada Research Press, 302 pp.
- Margulis, R.Ya. (1976) New genera of the sub-order Physophorae from the Indian Ocean. *Zoologicheskii Zhurnal*, 55, 1244–1246. [In Russian].
- Margulis, R.Ya. (1980) A redescription of *Tottonia contorta* and composition of the family Apolemidae (Siphonophora, Physophorae). *Zoologicheskii Zhurnal*, 59, 342–348. [In Russian].
- Medina, M., Collins, A.G., Silberman, J.D. & Sogin, M.L. (2001) Evaluating hypotheses of basal animal phylogeny using complete sequences of large and small subunit rRNA. *Proceedings of the National Academy of Sciences*, 98, 9707–9712. <http://dx.doi.org/10.1073/pnas.171316998>
- Medlin, L., Elwood, H.J., Stickel, S. & Sogin, M.L. (1988) The characterization of enzymatically amplified eukaryotic 16S-like rRNA-coding regions. *Gene*, 71, 491–499. [http://dx.doi.org/10.1016/0378-1119\(88\)90066-2](http://dx.doi.org/10.1016/0378-1119(88)90066-2)
- Östman, C. (2000) A guideline to nematocyst nomenclature and classification, and some notes on the systematic value of nematocysts. *Scientia Marina*, 64 (Supl. 1), 31–46. <http://dx.doi.org/10.3989/scimar.2000.64s131>
- Pugh, P.R. (1999) A review of the genus Bargmannia Totton, 1954 (Siphonophorae, Physonecta, Pyrostephidae). *Bulletin of the Natural History Museum. Zoology*, 65, 51–72.
- Sonnenberg, R., Nolte, A.W. & Tautz, D. (2007) An evaluation of LSU rDNA D1-D2 sequences for their use in species identification. *Frontiers in Zoology*, 4 (6), 12 pp.
- Stepanjants, S.D. (1967) Siphonophores of the seas of the USSR and the northern part of the Pacific Ocean. *Opredeliteli po Faune SSSR*, 96, 1–216. [In Russian].
- Totton, A.K. (1960) Studies on *Physalia physalis* (L.). Part 1. Natural History and morphology. *Discovery Reports*, 30, 301–368.
- Totton, A.K. (1965) *A Synopsis of the Siphonophora*. British Museum (Natural History), London, 230 pp., 20 Plates.
- Werner, B. (1965) Die Nesselkapseln der Cnidaria, mit besonderer Berücksichtigung der Hydrozoa. 1. Klassifikation und Bedeutung für die Systematik und Evolution. *Helgoländer Wissenschaftliche Meeresuntersuchungen*, 12, 1–39. <http://dx.doi.org/10.1007/bf01612091>

Erratum

<http://dx.doi.org/10.11646/zootaxa.3710.1.9>
<http://zoobank.org/urn:lsid:zoobank.org:pub:9F9E383D-7F39-4785-A7D2-01A7177B4A78>

STEFAN SIEBERT, PHIL R. PUGH, STEVEN H. D. HADDOCK & CASEY W. DUNN (2013) Re-evaluation of characters in Apolemiidae (Siphonophora), with description of two new species from Monterey Bay, California. *Zootaxa* 3702 (3), 201–232

The paper was published with the understanding that the video would be included as supplementary information. After publication it was found that *Zootaxa* policy does not allow videos as supplementary information. The authors have posted the video at a third party site, and the text should be amended as follows to reflect this change:

Page 205, line 11: "..supplementary video (Supplementary video)." should read "..supplementary video (at <http://dx.doi.org/10.7301/Z0WD3XH9>)."

Page 205, line 26: ".. outline (Supplementary Video)." should read "..outline (Supplementary video at <http://dx.doi.org/10.7301/Z0WD3XH9>)."

Page 213, line 47: "(Supplementary video, for Doc Ricketts D311-D4 specimen)." should read "(Supplementary video at <http://dx.doi.org/10.7301/Z0WD3XH9>, for Doc Ricketts D311-D4 specimen)."